1982-10

Instrumental photon activation analysis using the linear accelerator at the Naval Postgraduate School

Fisher, Wayne Alan

Monterey, California. Naval Postgraduate School

NAVAL POSTGRADUATE SCHOOL
Monterey, California

THESIS

INSTRUMENTAL PHOTON ACTIVATION ANALYSIS USING THE LINEAR ACCELERATOR AT THE NAVAL POSTGRADUATE SCHOOL

by

Wayne Alan Fisher

October 1982

Thesis Advisor: F. Buskirk

SECURITY CLASSIFICATION OF THIS PAGE (When Data Entered)

REPORT DOCUMENTATION PAGE

READ INSTRUCTIONS BEFORE COMPLETING FORM

1. REPORT NUMBER	2. GOVT ACCESSION NO. / 3. RECIPIENT'S CATALOG NUMBER
4. TITLE (and Subtitle): Instrumental Photon Activation Analysis Using the Linear Accelerator at the Naval Postgraduate School	5. TYPE OF REPORT & PERIOD COVERED: Master's Thesis, October 1982 / 6. PERFORMING ORG. REPORT NUMBER
7. AUTHOR(s): Wayne Alan Fisher	8. CONTRACT OR GRANT NUMBER(s)
9. PERFORMING ORGANIZATION NAME AND ADDRESS: Naval Postgraduate School, Monterey, California 93940	10. PROGRAM ELEMENT, PROJECT, TASK AREA & WORK UNIT NUMBERS
11. CONTROLLING OFFICE NAME AND ADDRESS: Naval Postgraduate School, Monterey, California 93940	12. REPORT DATE: October 1982 / 13. NUMBER OF PAGES: 107
14. MONITORING AGENCY NAME & ADDRESS(if different from Controlling Office)	15. SECURITY CLASS. (of this report) / 15a. DECLASSIFICATION/DOWNGRADING SCHEDULE

16. DISTRIBUTION STATEMENT (of this Report)

Approved for public release, distribution unlimited

17. DISTRIBUTION STATEMENT (of the abstract entered in Block 20, if different from Report)

18. SUPPLEMENTARY NOTES

19. KEY WORDS (Continue on reverse side if necessary and identify by block number)

Photon Activation Analysis, Fingerprinting of Oil, Analysis of Petroleum, Trace Element Analysis

20. ABSTRACT (Continue on reverse side if necessary and identify by block number)

Charcoal, charcoal residue, potting soil, aluminum foil, bismuth germanate, and petroleum samples have been investigated using instrumental photon activation analysis (i.e., no radiochemistry). The major and minor elements routinely observed by this nondestructive method were: C, Cl, Ca, Fe, Mg, Si, and K. A comprehensive review of the principles of IPAA was also included in the study. The principles were applied to a theoretical analysis of an oil sample in which the trace element concentrations were

DD FORM 1 JAN 73 1473 EDITION OF 1 NOV 65 IS OBSOLETE
S/N 0102-014-6601

SECURITY CLASSIFICATION OF THIS PAGE (When Data Entered)

known. It was concluded that IPAA is a highly sensitive technique which could be used to fingerprint oils.

Approved for public release, distribution unlimited

Instrumental Photon Activation Analysis Using the Linear Accelerator at the Naval Postgraduate School

by

Wayne Alan Fisher
Lieutenant, United States Coast Guard
B.S., United States Coast Guard Academy, 1977

Submitted in partial fulfillment of the
requirements for the degree of

MASTER OF SCIENCE IN PHYSICS

from the

NAVAL POSTGRADUATE SCHOOL
October 1982

ABSTRACT

Charcoal, charcoal residue, potting soil, aluminum foil, bismuth germanate, and petroleum samples have been investigated using instrumental photon activation analysis (i.e., no radiochemistry). The major and minor elements routinely observed by this nondestructive method were: C, Cl, Ca, Fe, Mg, Si, and K. A comprehensive review of the principles of IPAA was also included in the study. The principles were applied to a theoretical analysis of an oil sample in which the trace element concentrations were known. It was concluded that IPAA is a highly sensitive technique which could be used to fingerprint oils.

TABLE OF CONTENTS

LIST OF TABLES

LIST OF FIGURES

ACKNOWLEDGMENT

I would like to thank the following people for their contributions towards the completion of this thesis: Professor F. R. Buskirk and Professor J. N. Dyer for their advice and assistance as thesis advisors; Don Snyder for his help in the experimental portion of the thesis, in particular for running the linac; Professor Alan P. Bentz from the U. S. Coast Guard Research and Development Center for providing oil samples; Professor George A. Flanigan from the Coast Guard Central Oil Identification Laboratory for providing oil samples; and my wife, Linda, for her encouragement and support.

I. INTRODUCTION

Activation analysis is a widely used analytical procedure for the study of elements in a matrix. In most studies, thermal neutrons have been used because of the general availability of nuclear reactors and the large cross sections of many nuclides for thermal activation analysis. However, not all elements can be conveniently determined by neutron activation analysis. For example, carbon, nitrogen, oxygen, iron and lead are not highly activated by thermal neutrons. In other cases the (n,γ) reaction may result in a product which is stable. For these situations photon activation analysis may prove useful. In fact, photon activation offers several advantages as a complement to neutron activation. (a) As alluded to above the (γ,n), (γ,p), et cetera, reactions of target nuclides often lead to products other than those resulting from neutron activation. Thus there are more possibilities of forming products with half-lives and gamma ray energies convenient for analysis. (b) For a matrix which contains elements with very large thermal neutron cross sections, flux pertubations can cause errors in the procedure. This problem, known as self-shielding, is not as serious with photons as photons typically have longer ranges in samples than neutrons. (c) Finally, since photonuclear cross sections are a function of photon energy

it is possible to optimize certain photoreactions by judicious choice of the irradiating energy. This technique is not possible with neutron activation analysis.

Photon activation is the process involving nuclear reactions such as (γ,n), (γ,p), (γ,T), (γ,np), et cetera. The high energy gamma rays are usually produced by the collision of a high energy electron beam with a high Z material such as tungsten, which results in a broad frequency distribution of photons, called the bremsstrahlung spectrum. Reported values in the literature for electron beam energy range from 6-115 Mev and for beam current 5 uA to 1mA (See Table I).

Table I. Survey of Electron Beam Energies and Currents Used in Photon Activation Analysis

Principal Author	Electron Beam Energy Mev	Electron Beam Current uA	Reference
Kaminishi	6	1000	21
Chattopadhyay	15-44	25-225	12
Mulvey	22	250	22
Wilkens	22	30 or 45	23
Aras	30	50	15
Lutz	35	20	20
Hislop	35-40	5	1
Ricci	105-115	210	24

One of the attractive features of photon activation analysis (PAA) is its use as a nondestructive technique for multi-element analysis. This aspect along with other

characteristics of the method are discussed by Hislop in his review: PAA of biological and environmental samples [Ref. 1: p. 1159]. Included in the review is a table listing elements found in the following materials: tobacco, tree bark, hair, kale, blood, soil, bone, air particulates, and urine. Brazil nuts [Ref. 2: p. 99], rubber [Ref. 3] and moonshine whiskey [Ref. 4] have also been investigated using photons.

The focus of this study will be petroleum. The analysis of petroleum is motivated by a desire to use photon activation analysis as a technique to identify the source of an oil spill. It is known, for example, that the trace elements present in oil depend strongly on the source of the oil. The approach to be taken will be to first analyze environmental matrices such as charcoal and soil. The techniques developed are then extended to an exploratory analysis of petroleum.

II. THEORETICAL CONSIDERATIONS

A. GENERAL TECHNIQUE

The basic concept of either neutron or photon activation analysis is the production of radioactive nuclides as a result of some induced nuclear reaction. As the radioactive nuclide decays, selected radiations such as gamma rays are measured which will aid in the identification of the original elements in the sample. By judicious choice of the irradiation and counting variables it is possible to optimize the study of individual elements.

There are five general steps in activation analysis: (1) the selection of an appropriate nuclear reaction; (2) the preparation of samples for irradiation; (3) the irradiation; (4) the post-irradiation assays; (5) the evaluation of the experimental data. The general principles for each of these steps, as applied to photon activation analysis, will be reviewed here. More detailed discussions will follow in subsequent sections.

1. Nuclear reactions to be expected in photon activation are a function of the physical, chemical, and nuclear properties of the sample matrix and activation products. The two general situations are the investigation of a sample for known elements and the investigation of a sample for unknown elements. In either case the importance of interfering

and/or competing reactions must be considered. In selecting an optimum reaction a necessary condition is the availability of adequate sources of nuclear data.

2. One of the advantages of photon activation is that it usually requires little or no sample preparation. Specifically, pre-irradiation chemical processing is not done except in special applications. Samples to be irradiated may be pure elements or a mixture of elements either in solid or liquid form. The usual containers for irradiation are standard polyethylene vials and aluminum capsules.

3. The irradiation itself is accomplished with high energy photons. While there are a number of ways to produce photons the most common method is to use an electron linear accelerator. The variables of importance in the irradiation are the energy of the electron beam, the time of irradiation, the intensity of the irradiation, the number of target atoms and the geometry of the target. This method will be explained in more detail in Chapter II-C.

In general a higher irradiating energy will give higher yields. However, competing reactions will also be enhanced. Therefore photon activation experiments are most often done with a lower irradiating energy (20-40 Mev electron beam) and higher beam intensities (20-250 uA beam current), as compared

to the typical 100 Mev, 1uA beam produced by the Naval Postgraduate School Linac.

4. Post-irradiation assays are of two types: absolute or comparative. In the absolute assay accurate values of all variables (i.e., flux, cross sections, detector efficiency, et cetera) must be known. The comparative technique requires relative measurements only. In this method a sample and a standard are irradiated simultaneously. By taking the ratio of activities the need for certain nuclear data is eliminated. This gives more accurate results with more convenience than the absolute method. For this reason the comparative assay is used most often.

With either method suitable counting equipment is required for the type of radiation to be observed. Frequently NaI(Tl) or Ge(Li) detectors are used to record the gamma ray spectrum of the decaying radionuclides.

5. The final step in photon activation is the evaluation of the experimental data. For gamma ray spectroscopy this involves identifying the energy of the photopeaks observed in the gamma ray spectrum. When possible the half-life associated with a given photopeak should be measured. With this information photopeaks can be matched to particular radioisotopes and the original target nucleus deduced.

This final step should also include a discussion of the possible errors contributing to the accuracy and precision of the experiment.

B. NUCLEAR REACTIONS

A nuclear reaction occurs when a particle of sufficient energy interacts with a nucleus to induce a change in the nucleus. This process is different from the radioactive decay of a nucleus. A nuclear reaction is induced; radioactive decay is spontaneous.

A nuclear reaction is written as

$$A + a \longrightarrow B + b + Q$$

where A is the target nucleus, a is the irradiating particle, B is the product nuclide, b is the particle emitted from A, and Q is the change in energy of the system. A shorthand notation for the above reaction is

$$A(a,b)B$$

The irradiating particles can be neutrons, electrons, photons or ions. For photon activation there are two parameters of fundamental importance. These are the energy of the incoming photon and the cross section for the reaction.

The minimum photon energy for a reaction to occur is the threshhold energy. This is also called the separation energy by some authors since it is the energy at which a product nuclide begins to form. For (γ,n) reactions the threshholds

usually range from 7 to 18 Mev and they decrease with increasing atomic number [Ref. 5: p. 721].

The reaction cross section is a measure of the probability a reaction will occur. It has units of barns where 1 barn = 10^{-24} cm^2. Typical cross sections for photon reactions are on the order of millibarns. Like the threshhold energy, the cross section varies with the atomic number ranging from 1.6 millibarns for beryllium 9 to 1.58 barns for plutonium 239. Other cross section values can be found in the activation analysis handbook by R. C. Koch [Ref. 6].

The reaction cross section is also a function of the photon energy. For example, as the photon energy is increased in a (γ,n) reaction there is a greater chance that competing reactions will occur (i.e. (γ,p), (γ,np), (γ,2n), et cetera. The result is a marked decrease in the cross section for (γ,n). This phenomenon is known as the giant resonance and is pictured qualitatively in Figure 1. E_T is the threshhold energy, σ_M the maximum cross section, and E_o the resonance energy.

Both the maximum cross section and the resonance energy are found to vary smoothly with the mass number from sodium to uranium. They are roughly proportional to NZ^2/A and $A^{-0.33}$ respectively [Ref. 7: p. 9]. A more exact expression for the resonance energy is given by DeSoete [Ref. 5: p. 728].

$$E_o = 40.7\ A^{-0.20}$$

The maximum cross section for $2 < Z < 20$ varies between 1 and 30 millibarns. For $20 < Z < 83$ the peak cross section can be estimated by:

$$\sigma(E_o) = 8.15Z - 156.4 \text{ mb}$$

Figure 2 displays the threshhold energy and resonance energy as a function of atomic number. It can be seen that the most efficient range of photon energies for activation purposes is 15-25 Mev.

For low Z nuclides the (γ,n) and (γ,p) nuclides are of the same order of magnitude. However as Z increases the coulomb barrier of the nucleus hinders the emission of a proton [Ref. 5: p. 723]. Therefore the (γ,n) reaction is more probable for $Z > 30$.

The nuclear reactions applicable to photon activation analysis are of two types. The first type are (γ,γ^1) reactions which lead to isomeric states of an element. The threshhold for these reactions are usually well below 10 Mev. Because the excited nucleus decays back to the ground state by emitting a characteristic gamma, the (γ,γ^1) reaction is attractive for both its selectivity and its non-destructive feature.

The second type of reaction includes (γ,n), $(\gamma,2n)$, et cetera reactions where neutrons are ejected from the nucleus

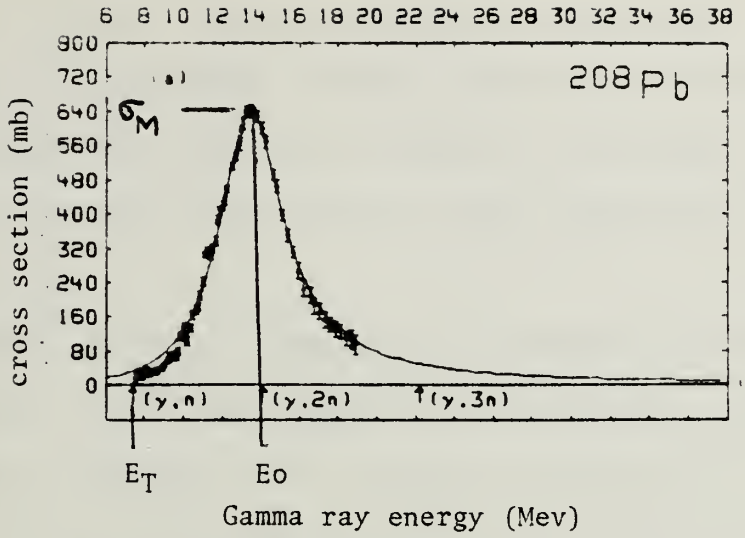

Figure 1. Giant Dipole Resonance of Pb208 [Ref. 25: p. 736]

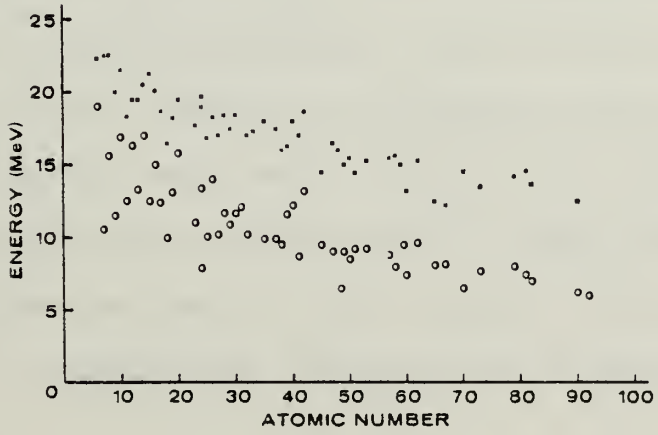

o Threshhold energy
x Maximum cross section energy

Figure 2. Threshhold Energy and Energy of Maximum Cross Section for (γ,n) Reactions [Ref. 8: p. 95]

and (γ,p), (γ,T), (γ,np), et cetera, reactions where charged particles are emitted. These reactions are considered primary reactions, that is, a nuclear reaction induced in an original sample element by the principle irradiating particle.

Besides primary reactions, secondary and second order reactions are also possible in photon activation. A secondary reaction is a nuclear reaction in an original sample constituent by particles created during primary reactions. A common reaction would be a (n,γ) event. In this case neutrons produced from (γ,n) reactions may react with nuclei from the original sample.

Second order reactions are of two types. The first type is one in which the principle irradiating particles interact with primary reaction products. Fortunately, this type of interference is not expected with photons since the reaction cross sections are very small [Ref. 6: p. 10]. The second type of second order reaction occurs when primary products undergo spontaneous decay. This type of interference may be important if neighboring elements of a matrix are being analyzed.

To summarize nuclear reactions, it can be expected that with increasing photon energy a number of gamma reactions are possible. Which one will predominate is a function of photon energy, photon flux, reaction cross sections, abundance of

target nuclides and the length of irradiation. An excellent review of many reactions possible with photon activation analysis is given by Toms [Ref. 9, 10]. Figure 3 is a display of possible primary gamma reactions.

C. PRODUCTION OF PHOTONS

There are four sources of photons for activation analysis: positron annihilation, nuclear reactions, radioactive isotopes and electron accelerators. Generally the least useful of these methods is positron annihilation, since the photon flux is about 10^{-4} to 10^{-5} times less than the bremsstrahlung flux available from electron accelerators [Ref. 11: p. 10].

The early work in photon activation analysis was accomplished with either natural or artificial radioisotopes. Borshov and co-workers, for example, in the late 1930's determined beryllium by prompt neutron emission with a radium source [Ref. 8: p. 93]. Other radioisotopes used to generate photons are Na24, Co60, and Sb124. Strengths of the sources range from 0.2 to 30,000 curies.

Production of photons by nuclear reactions is also possible. Del Bianko, for instance used monochromatic gamma rays from the $H^3(p,\gamma)\ He^4$ reaction to study photonuclear cross sections [Ref. 7]. Two other possible reactions are $Li^7(p,\gamma)Be^8$ and $B^{11}(p,\gamma)C^{12}$. The gamma ray fluxes obtained

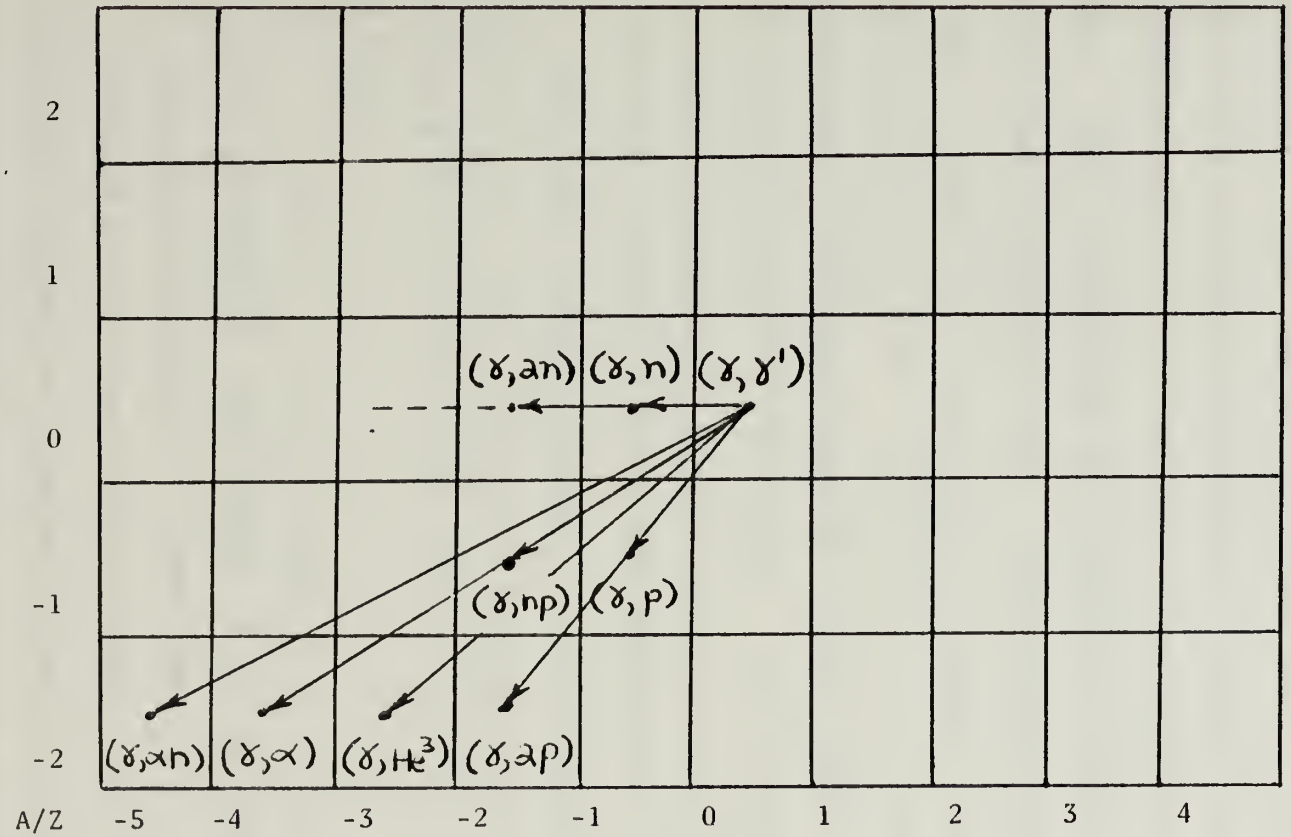

Figure 3. Possible Gamma Reactions

from these reactions, however, are very small and the gamma energy is fixed [Ref. 5: p. 732].

The fourth method of producing photon fluxes is by colliding a high energy electron beam with a high atomic number material. The inelastic scattering of the energetic electrons by the coulomb attraction of the positively charged target nucleus leads to the emission of a continuous spectrum of photons. This process and the radiation produced is known as bremsstrahlung (braking rays). The maximum energy for the gamma rays is equal to the highest kinetic energy of the irradiating electrons. Besides radiative losses (bremsstrahlung), electrons passing through matter also lose energy by excitation and ionization. This process has two effects. One, it results in the heating of the target and/or sample. Two, the number of electrons converted to photons is reduced. For thick targets (length > 1.5 radiation lengths) the fraction of the electron energy converted to bremsstrahlung can be calculated from an expression given by Koch and Motz:

$$\epsilon = 1 - \ln(1 + 1.2 \times 10^{-3} EZ)/1.2 \times 10^{-3} EZ$$

where ϵ is the fractional efficiency, A is the atomic number and E is the electron energy in Mev [Ref. 8: p. 94]. For lead (Z = 82) and E = 100 Mev electron beam, ϵ = 75%.

An important feature of bremsstrahlung is its anisotropic character as the produced gamma rays are peaked forward

[Ref. 5: p. 732]. The number of photons in the forward direction increases with increasing electron energy. The angular width is roughly $1/\gamma$ in radians, where $\gamma = E((\text{electron})/mc^2)$.

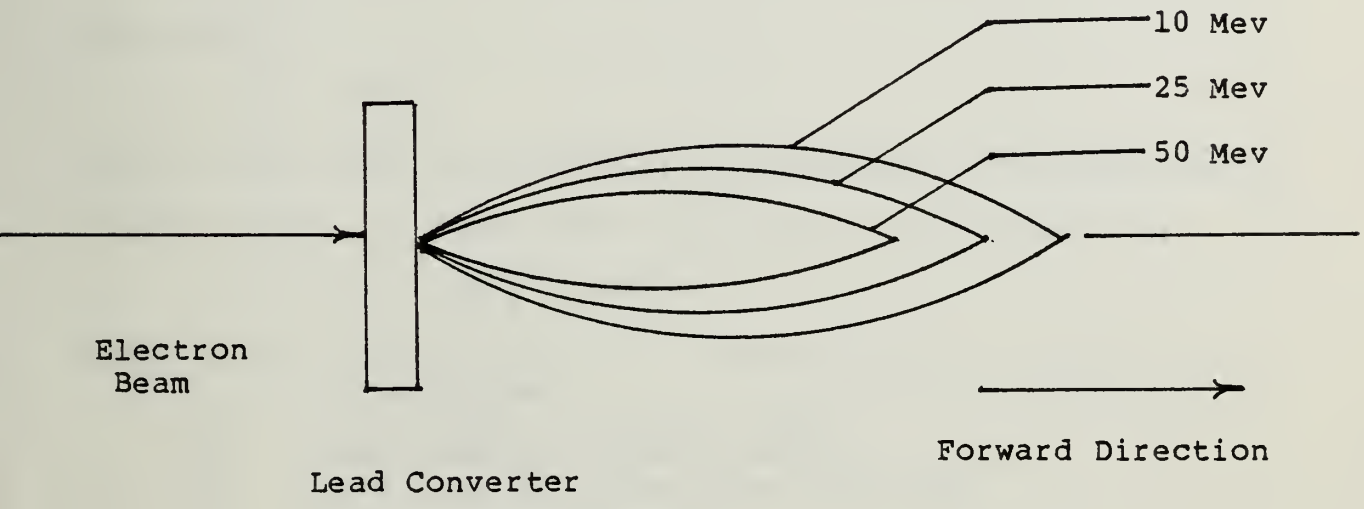

Figure 4. Schematic Sketch to Illustrate the Spatial Distribution of Bremsstrahlung

Van de graaff generators, synchrotrons, betatrons, microtrons, and linear accelerators are all capable of producing electron beams for use in bremsstrahlung. The most commonly used apparatus for photon activation, however, is the linear accelerator. This is because a requirement for trace analysis is a high intensity beam. Chattopadhyay and Jervis recommend a photon flux of about 10^{13} to 10^{14} photons/cm^2/sec. [Ref. 12: p. 1639]. DeSoete, et. al. suggest that an integrated current of more than 10 uA and energies up to 40 Mev be used for activation analysis

[Ref. 5: p. 278]. These levels of intensities and energies are easily obtained with most linear accelerators.

D. ACTIVATION EQUATION

The activation equation in its simplest form can be expressed as

$$(1) \quad A \propto W$$

which states that the activity of an element is proportional to its weight. In more detail equation (1) is written as

$$(2) \quad A(o) = N\sigma\phi(1-e^{-\lambda T})$$

where $A(o)$ = the activity of a radionuclide at the end of an irradiation
N = the number of target atoms
σ = the reaction cross section
ϕ = the flux of irradiating particles
λ = the decay constant
T = the irradiation time

For a particular radionuclide equation (2) is modified to account for the fractional abundance, f, of the isotope being analyzed.

$$(3) \quad A(o) = \frac{Wf}{M}\sigma\phi(1-e^{-\lambda T})\ N_o$$

Here the number of target atoms has been expressed as $W/M\ N_o$ where W is the weight of the element present in the sample, M is its atomic weight, and N_o is Avogadro's number.

Usually the activity will not be determined until some time t after the irradiation. Therefore another factor must be added to equation (3) to account for the radioactive decay of the isotope being measured. The activity is then

$$(4) \quad A(t) = \frac{Wf}{M}\sigma\phi(1-e^{-\lambda T})\ e^{-\lambda t}\ N_o$$

This equation is rearranged to yield

$$(5) \quad W = \frac{MA(t)e^{\lambda t}}{f\sigma\phi(1-e^{-\lambda T})N_o}$$

In theory if all the variables on the right hand side of equation (5) are known then the weight of an element can be calculated directly. This is an example of an absolute assay. In practice there is enough uncertainty in the reaction cross section and flux that in most cases a comparative technique is used.

As explained previously, the comparative assay involves the simultaneous irradiation of a sample and a standard. Using equation (5) the weights of a desired element in a sample X and a standard S are

$$(6a) \quad W_x = \frac{MA_x(t_x)e^{\lambda tx}}{f\sigma\phi(1-e^{-\lambda T})N_o}$$

$$(6b) \quad W_s = \frac{MA_s(t_s)e^{\lambda ts}}{f\sigma\phi(1-e^{-\lambda T})N_o}$$

Assuming a homogeneous irradiation of the sample and standard the ratio of W_x/W_s gives

$$(7) \quad \frac{W_x}{W_s} = \frac{A_x(tx)e^{\ tx}}{A_s(ts)e^{\ ts}}$$

The activities in equation (7) are determined experimentally by counting the sample and standard under comparable conditions. W_s is known, so W_x can then be calculated.

1. Sensitivity Calculation

A modified equation (5) can be used to measure the sensitivity of an element for activation analysis. The minimum weight of an element detectable in an irradiated sample is

$$(8)\quad W_{min} = \frac{MAm(t)e^{\lambda t}}{f\sigma\phi(1-e^{-\lambda T})N_o Y F \varepsilon}$$

where M = atomic weight of the element
Am(t) = minimum detectable counting weight at the time of counting
$e^{\lambda t}$ = decay from end of irradiation to start of counting
f = isotopic abundance
σ = reaction cross section
ϕ = irradiation flux
$1-e^{-\lambda T}$ = saturation factor for the length of the irradiation
Y = chemical yield if radiation chemistry is used
F = self absorption losses
ε = overall counting efficiency

A few of these variables merit additional comments. Am(t) is the minimum resolvable counting rate above background and is often assumed to be 2B where B is the background [Ref. 13: p. 242].

The overall counting efficiency is given by

$$\varepsilon = \frac{Ci}{D}$$

where Ci is the number of counts of radiation i and D is the number of disintegrations of the nuclide in the same time interval [Ref. 13: p. 243]. It depends both on the radiation-energy efficiency of the detector and on the decay scheme of the radioisotope being measured. For example a

NaI(Tl) detector may have a 20% efficiency for 2.13 Mev gamma rays, but the radioisotope Cl34m decays only 40% of the time with the emission of 2.13 Mev gamma rays. The overall counting efficiency is then

$$\epsilon = 0.20 \times 0.40 = 0.08$$

The counting geometry will affect the overall counting efficiency. Usually it is determined from a calibration curve of ϵ vs gamma ray energy for a fixed set of counting conditions.

From equation (8) it can be seen that the maximum sensitivity (i.e., minimum weight) is obtained when the variables in the numerator are minima and the variables in the denominator are maxima. As an example of the sensitivity calculation, an activation analysis for the determination of lead in petroleum will be evaluated. The 0.899 Mev photopeak from the Pb206(γ,2n)Pb204m reaction is used for analysis.

1. Counting system:
   NaI(Tl) detector, total B(photopeak) = 17 cpm
   Am(t) = 34 cpm = .568 cps
   overall counting efficiency = 32%

2. Post-irradiation processing:
   elapsed time to counting : 3 hours
   Y = 1 (no chemical processing).
   F = 1 (no self absorption).

3. Irradiation conditions:
   σ = 85 mb
   $\phi = 2 \times 10^{13}$ photons/cm^{2}sec.
   irradiation time = 1 hour

4. Sample data:
isotopic abundance of Pb206 = .236
sample size = 1 gram oil
assume no major interfering constituents.
atomic weight of lead = 207.2 g/mole.
$\lambda = .0108\ min^{-1}$

Equation (8) yields:

$$W_{min} = \frac{207.2(.568)e^{.0103(180)}}{.236(85\times10^{-27})(2\times10^{13})(1-e^{-.0103(60)})(6.02\times10^{23})(.32)}$$

$$W_{min} = 2.1 \times 10^{-8} \text{ grams}$$

Usually it is the concentration of an element in a sample which is desired rather than the absolute amount in the sample. This concentration is obtained by dividing W_{min} by the sample weight and multiplying by 10^6 for ppm and 10^2 for percent.

$$(9a)\quad C_{min} = \frac{W_{min}}{S} \times 10^6 \text{ ppm}$$

$$(9b)\quad C_{min} = \frac{W_{min}}{S} \times 10^2\ \%$$

For the above calculation the concentration of lead which could be determined in a sample under the stated conditions would be .021 ppm. Although this is an idealized calculation because no interfering reactions were assumed, the excellent sensitivity calculated is not unreasonable for activation analysis. Sensitivities of nanograms are frequently reported in the literature for activation analysis.

E. GAMMA RAY SPECTROSCOPY

The most common method for collecting data in photon activation analysis is to use either a NaI(Tl) or Ge(Li)

detector coupled to a multichannel analyzer. To evaluate the gamma ray spectrum obtained it is helpful to understand the basic principles of gamma ray spectroscopy. This section will be a review of those principles.

Not considering cost, the choice of using either a NaI(Tl) or Ge(Li) detector is driven by the type of analysis to be done. Both detectors have advantages. For example, the Ge(Li) crystal has an intrinsic high resolution. The spectrum obtained is characterized by very narrow peaks (typically less than 1/10 the width of NaI peaks) that lie on relatively simple continuous compton distributions [Ref. 14: p. 636]. The peaks are thus widely separated and completely non-interfering. A Na24 spectrum obtained with a NaI(Tl) and a Ge(Li) detector is compared in Figure 5. However, the efficiency of the Ge(Li) crystal is only a small fraction of the NaI(Tl) crystal. A representative number would be 6-10% compared to a standard NaI(Tl) crystal. Thus the choice of a detector is a compromise between resolution and efficiency. For low level counting of a single element in a relatively simple matrix, high efficiency is needed and hence NaI(Tl) would be the preferred choice. For multielement analysis of complex environmental or biological samples resolution is the most important criterion and Ge(Li) detectors must be used. Regardless of which detector is used, the general operating principle is the same.

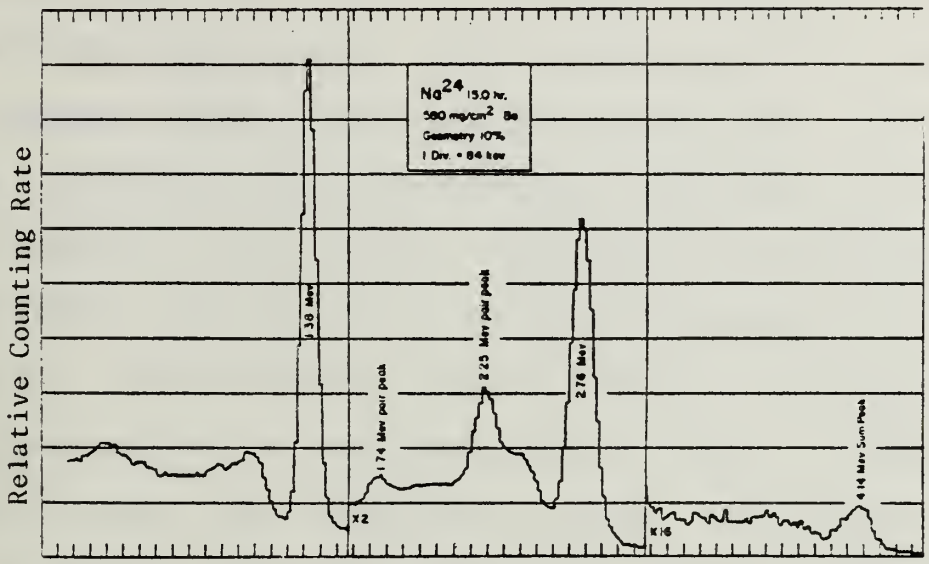

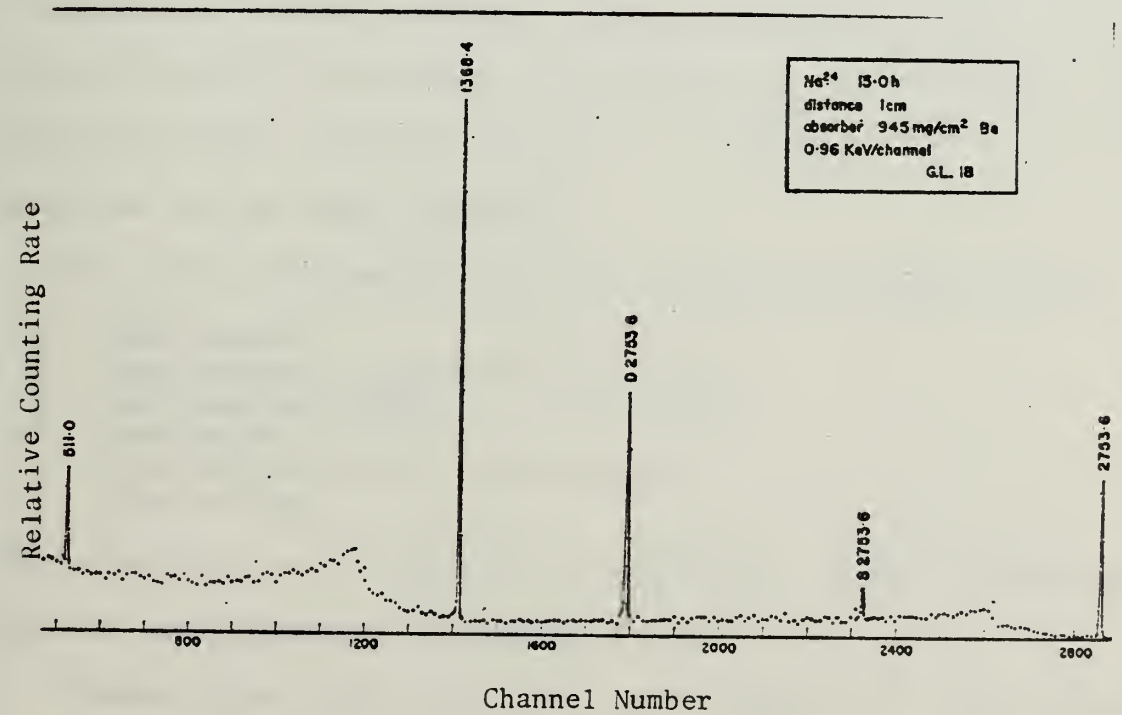

Figure 5. Comparison of Na24 Spectra Taken with NaI(Tl) and Ge(Li) Detectors [Ref. 26]

Gamma rays interact in a crystal (NaI(Tl) or Ge(Li)) in essentially three ways: (1) the photoelectric effect, (2) the compton effect, and (3) pair production. All three of these interactions produce secondary electrons which deposit their energy in the crystal, resulting in a scintillation in the NaI(Tl) crystal and an electronic pulse in the Ge(Li) crystal. With NaI(Tl), the crystal is coupled via a photocathode to a photomultiplier tube to convert the scintillations into electronic pulses. With both crystals, the electronic pulses are amplified, sorted by amplitude, and stored in a pulse-height analyzer. Since the pulses are proportional to the incident energy deposited in the crystal, the end result is a gamma ray spectrum. If more than a few radionuclides are decaying in a sample, the resulting spectrum can be very complex.

The major characteristics of a gamma ray spectrum are:

a. photopeaks
b. the compton edge and distribution
c. backscatter peaks
d. sum peaks
e. single and double escape peaks
f. tube noise.

These peaks are illustrated in Figure 6. Their origins can best be explained by discussing Figure 7.

Gamma rays with energies up to about 0.1 Mev interact within a NaI(Tl) crystal predominantly by the photoelectric effect. The photoelectric effect is a direct interaction of photons with the orbital electrons in an atom. Up to about

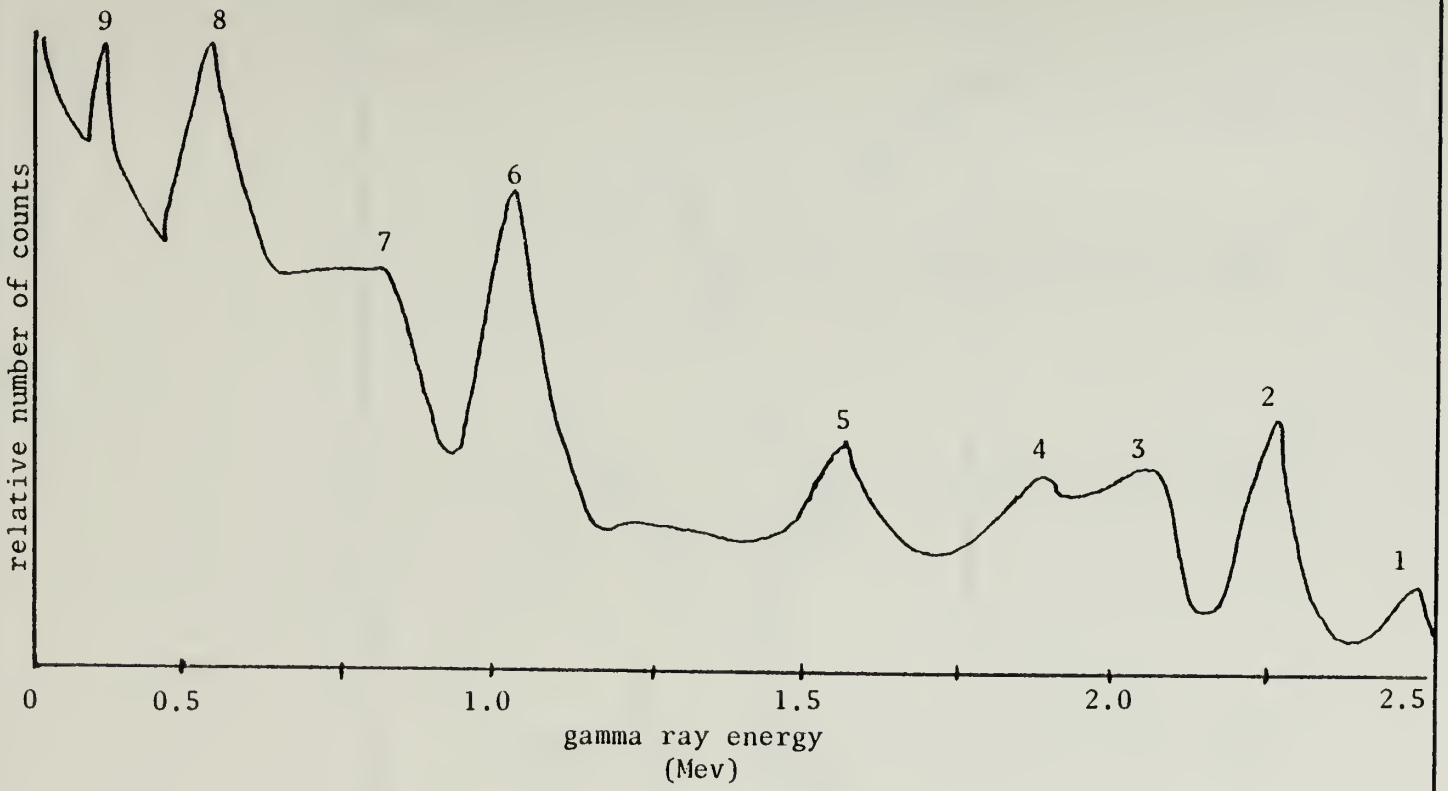

KEY:
1. sum peak (1.0 + 1.5) Mev
2. photopeak at 2.25 Mev
3. compton edge
4. single escape peak from 2.
5. double escape peak from 2.
6. photopeak at 1.0 Mev
7. compton edge
8. annihilation radiation .511
9. backscatter peak from surroundings

Figure 6. Hypothetical Gamma Ray Spectrum

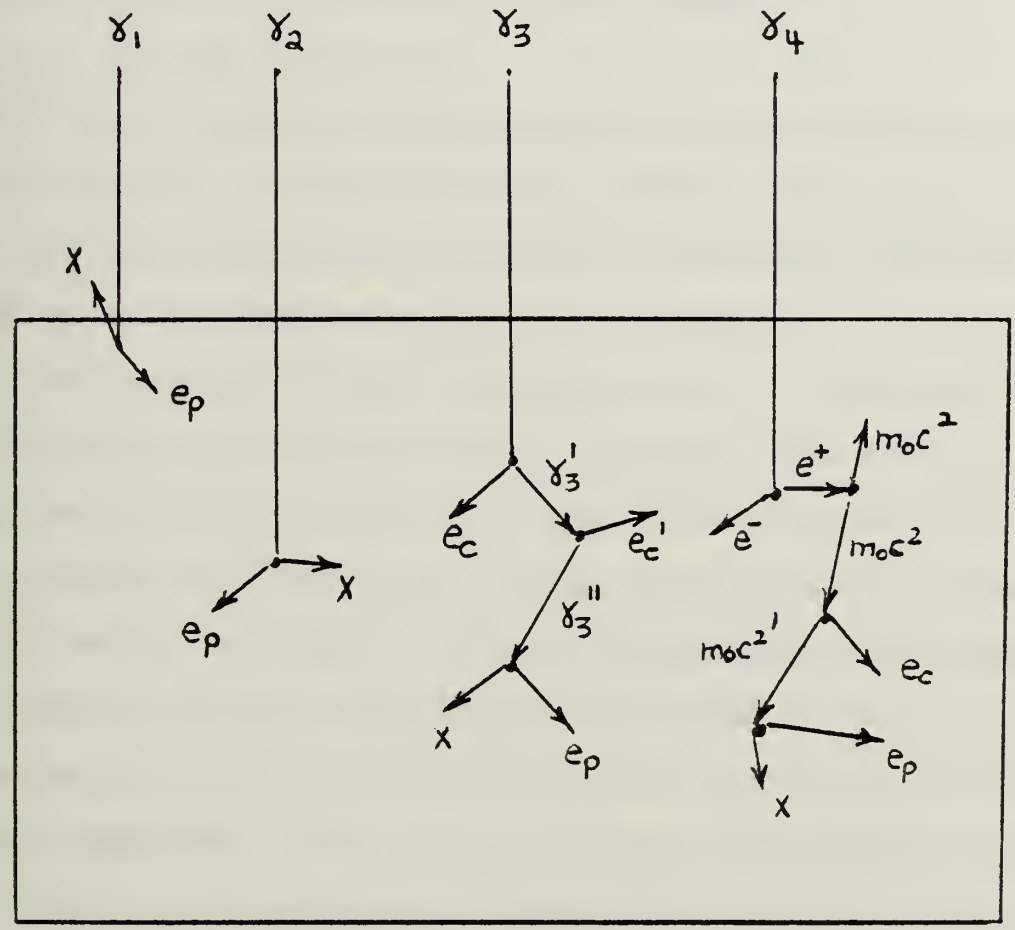

Figure 7. Interactions of Gamma Rays with a NaI(Tl) Crystal [Ref. 14: p. 640]

0.5 Mev this effect is proportional to Z^5, so in NaI(Tl), the photons interact mostly with the iodine atoms. This is an inelastic collision the result being the ejection of an electron from the atom with kinetic energy.

$$(1) \quad E_e = E_\gamma - B_e$$

where B_e is the binding energy of the ejected electron in its orbital shell. The iodine atom will be left with a vacancy in its K shell which when filled by cascading electrons gives rise to a characteristic x-ray of 0.028 Mev.

The energy of the photoelectron in equation (1) is quickly deposited in the NaI(Tl) crystal. The K x-ray may or may not deposit its energy in the crystal depending on where the interaction took place. Both possibilities are depicted by γ_1 and γ_2 in Figure 7. If the interaction occurs near the surface the K x-ray may escape the crystal. If the interaction occurs elsewhere in the crystal the K x-ray is almost always captured. Thus, at low gamma ray energies two peaks can occur in the gamma ray spectrum: one at the incident gamma ray energy and one at 0.028 Mev below this. Because the difference between these two peaks is small in absolute magnitude, these two peaks are not observed separately at gamma ray energies above 0.170 Mev [Ref. 14: p. 641]. Only one peak would then occur at a pulse height corresponding to the incident gamma ray energy. This total absorption of the incident gamma ray represents the photopeak.

The next important process contributing to the formation of a gamma ray spectrum is the compton effect. This effect is similar to the photoelectric effect. However, an elastic rather than an inelastic collision occurs between the incident gamma ray and an electron. A compton electron will be the result from this collision and the gamma ray will emerge from the collision in a new direction and with reduced energy. This degraded gamma ray can then undergo additional compton scatterings or interact by the photoelectric effect. This process is illustrated by γ_3 in Figure 7. The total energy deposited in the crystal due to γ_3 would be $e_c + e_c' + e_p + x$. The total time for these interactions is so fast compared to the decay time of a light pulse from the NaI(Tl) detector that only one light pulse corresponding to the photopeak will be emitted by the crystal [Ref. 14: p. 642].

By solving the energy and momentum equations for the compton effect, the kinetic energy of the compton electron, T, and the energy of the scattered photon, E', can be expressed as

$$(2a) \quad T = \frac{E_o}{1 + \frac{m_o c^2}{(1-\cos\theta) E_o}}$$

$$(2b) \quad E^1 = \frac{E_o}{1 + \frac{(1-\cos\theta) E_o}{m_o c^2}}$$

where E_o is the energy of the incoming photon, $m_o c^2$ is the rest energy of the electron, and θ is the angle through which

the photon E' is scattered relative to the original direction of the photon E_o. From equation (2a) it is evident that as E^1 approaches 0, T approaches 0. That is to say, there is no minimum kinetic energy for the compton electron. However a maximum exists at $\theta = 180^o$.

$$(3a) \quad T_{max} = \frac{E_o}{1 + \frac{m_o c^2}{2E_o}}$$

The corresponding photon energy for $\theta = 180^o$ is given by

$$(3b) \quad E^1_{min} = \frac{E_o}{1 + \frac{2E_o}{m_o c^2}}$$

Referring back to the case of γ_3 in Figure 7, it is possible for the scattered photon γ_3' or γ_3'' to escape from the crystal. If this situation occurs an energy of $E_o - E'$ is deposited in the crystal. Since E' can vary from E_o when $\theta = 0$ to $E_o - T_{max}$ (when $\theta = 180^o$) a continuous distribution of peaks will appear in the gamma ray spectrum from 0 to T_{max}. T_{max} is called the compton edge.

The final mechanism important in gamma interactions is pair production. This event usually occurs in the coulomb field of the nucleus and in the process the gamma ray disappears and an electron positron pair is created. The minimum gamma ray energy for pair production to occur is 1.02 Mev (twice the rest mass energy of an electron). Pair production processes become significant in NaI(Tl) when the initial gamma ray energy is greater than 2 Mev.

γ_4 in Figure 7 illustrates the possible events which can occur in pair production. The energy of the electron in the electron-positron pair is quickly deposited in the crystal. The positron readily annihilates with an electron. This interaction produces two photons of .511 Mev traveling at an angle of 180° to one another in an arbitrary reference frame. These two photons may then interact by the compton or photoelectric process, or one or both may escape from the crystal. If neither photon escapes then a photopeak will appear in the gamma ray spectrum corresponding to the energy of γ_4. If one .511 Mev photon escapes a peak will form at the energy γ_4 - .511 Mev. This peak is called the single escape peak. If both .511 Mev photons escape from the crystal then a double escape peak forms at γ_4 -1.02 Mev. Continuous compton distributions are also present for each peak.

Another peak possible in a gamma spectrum is the sum peak. This occurs when the detector counts two gamma rays as one. These peaks become noticeable if the counting rate is high.

Besides the photopeaks, compton distributions, single and double escape peaks, and sum peaks produced by direct interactions of gamma rays from a source, secondary effects due to the inevitable surroundings tend to distort a gamma

ray spectrum. The various events possible are shown in Figure 8.

Compton scattering of the primary radiation from the surrounding material contributes to the pulse height distribution from zero amplitude to a maximum depending on the angle of scattering. The most common effect is backscattering (i.e. 180^{o} scattering) behind the source. The theoretical location of the backscatter peak is

$$E_{BS} = E_{o} - T_{max}$$

where E_{BS} is the energy of the backscatter peak and E_{o} and T_{max} are the incident gamma ray energy and compton edge respectively.

Annihilation radiation at .511 Mev is also common in a spectrum especially if a source decays by positron emissions. Pair production in the shielding material will also produce annihilation radiation.

The last probable interference from surrounding materials are x-rays produced by the photoelectric effect. A .074 Mev peak corresponding to the Pb x-ray is common.

Finally, tube noise from thermionic emissions and natural background from cosmic rays and surrounding radioactive materials complete the contributions to a gamma ray spectrum.

In summary, a spectrum typically consists of the following: photopeaks, compton distributions, single and double escape peaks, sum peaks, backscatter peaks, and noise

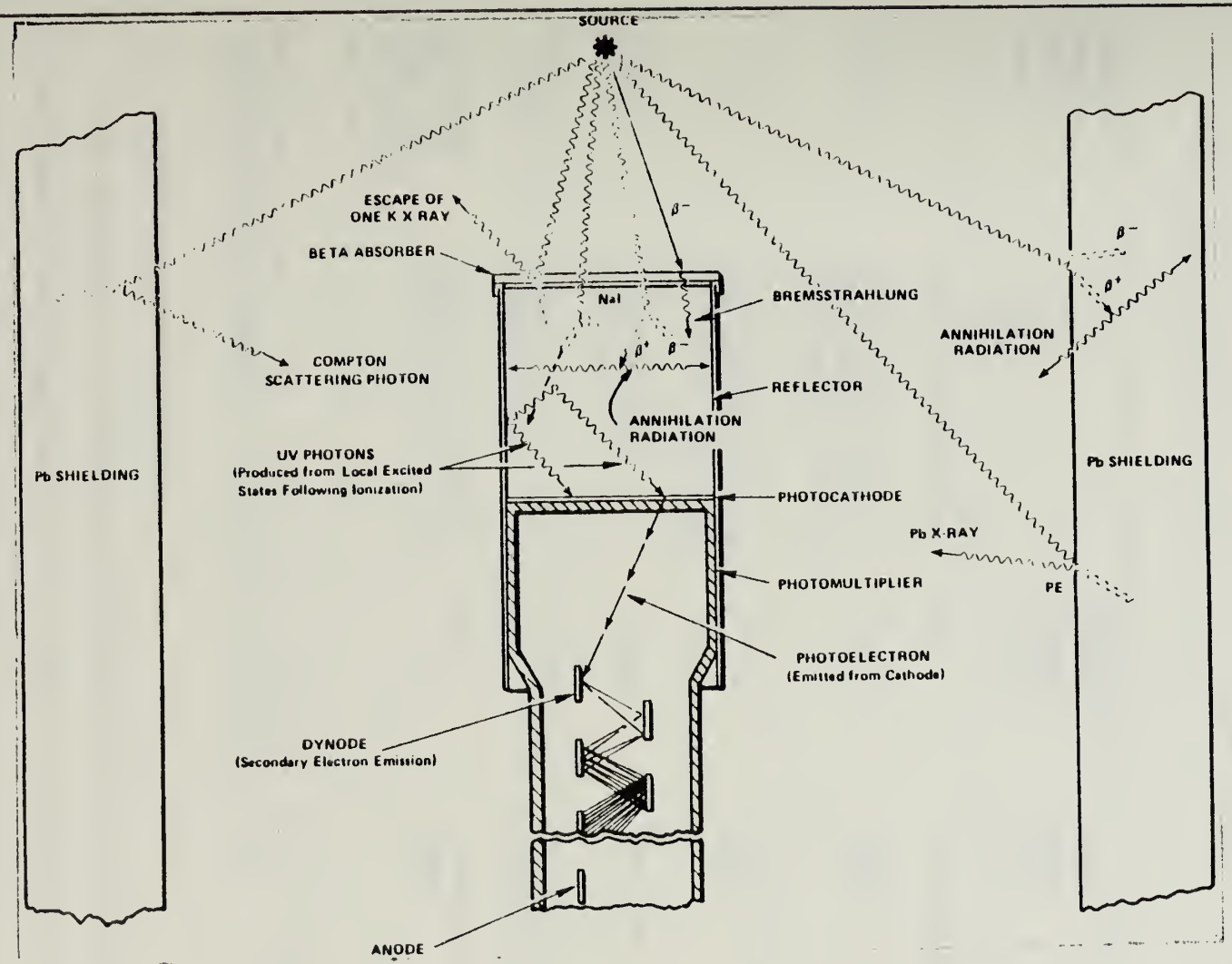

Figure 8. Summary of Nuclear Events in the Vicinity of a NaI(Tl) Detector [Ref. 27: p. 17]

effects. Table II and Figure 6 summarize the above discussion.

Table II. Origin of Peaks in a Gamma Ray Spectrum

Photon Escape Energy (Mev)	Origin	Spectrum Peak Energy (Mev)	Spectrum Peak Name
0	Total absorption	E_o	Photopeak
0.511	Pair production and escape of one .511 Mev photon	E_o-0.511	Single escape peak
1.02	Pair production and escape of two .511 Mev photons	E_o-1.02	Double escape peak
E^1_{min}	Compton 180° scattering	T_{max}	Compton edge
E^1_{min} to E_o	Compton scattering	0 to T_{max}	Compton distribution
E_o with E_{BS} re-entering	External Compton 180° scattering	E_{BS}	Backscatter peak

Adapted from J. B. Birks, The Theory and Practice of Scintillation Counting, Macmillan, 1964, p. 470.

F. PRECISION AND ACCURACY

The emphasis on precision and accuracy in the analysis of experimental data depends on the type of analysis to be done. For example, a very accurate result was required by Guinn and co-workers for their determination of lead in moonshine

whiskey for forensic purposes [Ref. 4]. However, in their exploratory studies of biological samples, drugs, glass, soil, and paper, the main effort was required for the identification of the elements found in the samples. Thus a rigorous error analysis was not required, implying less overall accuracy for the procedure.

In general, the need for precision and accuracy can be divided into four categories, according to the question to be answered [Ref. 13: p. 240].

1. Qualitative: is element Z present in the sample?

2. Threshhold: is element Z present in amounts greater than some given amount?

3. Relative: is element Z present in small or large amounts?

4. Quantitative: exactly how much of element Z is present in the sample? The greatest need for precision and accuracy is when quantitative results are required.

There are a number of errors in photon activation analysis which affect the overall accuracy. The main two are: (1) changes in the irradiation conditions, and (2) interfering nuclear reactions. These errors and other sources of errors are summarized in Table III.

Changes in the irradiation conditions refers to flux gradients in the sample. Careful attention to the sample geometry and close monitoring of the irradiating beam energy will minimize this type of error.

Table III. Sources of Error in Photon Activation Analysis[1]

Source	Estimated Error
	%
1. Chemical	
a. Sample weight	±1
b. Standard weight	±2
c. Yield (if seperation used)	±2
2. Irradiation	
a. Irradiation time (< 1 min)	±3
b. Nonhomogeneity of photon flux	±2
c. Electron beam energy	±1
3. Nuclear data	
a. Half-life	±2-10
b. Decay scheme	±2-50
c. Cross section	±5-30
4. Nuclear reactions	
a. Competing	Variable
b. Interfering	Variable
5. Counting	
a. Detector calibration	±3
b. Counting rate < 10^3 dps	±4
c. Geometrical factors	±1

[1] Adapted from J. P. Call, et. al., "The Accuracy of Radioactivation Analysis", in Modern Trends in Activation Analysis (Texas A & M University, College Station, 1965), pp. 258-258..

Interfering nuclear reactions occur when the same radionuclide is produced by more than one mechanism. An example is the production of Na24 by the following reactions.

$$Mg25(\gamma,p)Na24$$

$$Al27(\gamma,He^3)Na24$$

This type of interference can be reduced or eliminated by the proper choice of irradiating energy. For example, the threshhold energy for the (γ, He^3) reaction for Al27 is 23.7 Mev. Thus by using 20 Mev electrons to produce a bremsstrahlung flux of photons, no Na24 will be produced from Al27.

Another type of interference probable in photon activation analysis is overlapping gamma rays in the gamma ray spectrum. Various techniques are used when this type of interference occurs. If, for example, the interference is due to a short lived nuclide, the contribution of the short lived nuclide to the photopeak is minimized (if not eliminated) by waiting five half-lives before counting. On the other hand, if a long lived nuclide interferes, it can be produced in smaller quantity by limiting the length of the irradiation.

When all possible sources of errors are minimized, the overall accuracy of photon activation analysis is around ± 10%. A value of ±10 to ±15% is given by Aras, et. al. for their analysis of atmospheric particulate material [Ref. 15: p. 1407]. Chattopadhyay and Jervis estimated that the total error involved in analysis can be restricted to ±7 to ±8% in some instances, and to ±10% in all cases [Ref. 12: p. 1638].

III. EXPERIMENTAL PROCEDURES

A. GENERAL

The experiments done for this thesis can be classified in one of two groups. The first group involves experiments done with petroleum samples. The second group includes other environmental samples such as charcoal, charcoal residue, aluminum foil, soil, and a crystal of bismuth germanate (BGO).

Certain experimental conditions were constant for all experiments. In all cases except BGO, samples were irradiated with a bremsstrahlung flux of photons produced by the collision of a high energy electron beam with a 5.3mm thick lead target. The electron beam was generated by the Naval Postgraduate School's electron linear accelerator. The Linac is capable of producing electron energies between 20 and 100 Mev. The typical beam intensity was 5×10^{11} electrons/second.

Gamma rays emitted from radionuclides produced in the irradiation were counted with a 3 inch x 3 inch hermetically sealed Harshaw NaI(Tl) detector. The FWHM range for the 0.667 Mev gamma of Cs-137 was measured as .060 Mev, implying 9% resolution. For the 1.332 Mev gamma of Co-60 the FWHM value was .084 Mev for 6.3% resolution.

Pulses from the NaI(Tl) detector were amplified with an ORTEC 485 amplifier and then sorted and stored by a TRACOR NORTHERN 7200 multichannel analyzer. A two point energy calibration program of the multichannel analyzer made it easy to identify the gamma ray energies corresponding to all photopeaks. When possible the half-life associated with a given photopeak was measured.

B. COLLECTION OF SAMPLES

Samples were collected from a variety of sources. The charcoal sample was obtained by crushing a briquette of Kingsford "Match Light". The charcoal residue was also Kingsford's although after the barbecue. Two types of aluminum foil were used: Safeway and Reynolds Wrap. The soil sample was a commercial potting soil purchased locally. The BGO crystal analyzed was a fragment of a larger BGO crystal obtained from Harshaw Chemical Corporation. Finally, the oil samples came from one of three sources. Approximately 50 grams of used engine oil from a fried's car was contributed for analysis. Another 34 samples consisting of 12 crude oils, 6 lube oils, 6 #6 fuel oils, 3 bunker fuel oils, 6 #2 fuel oils, and 1 #5 fuel oil were provided by the U.S. Coast Guard's Central Oil Identification Laboratory. Five crude oils were also available for analysis from the U.S. Coast Guard Research and Development Center, Groton, Connecticut.

C. IPAA -GENERAL SAMPLES.

1. Aluminum Foil

As a check on the homogeneity of an irradiation, it is advisable to use a flux monitor. A suitable material to use in major and minor element analysis is household aluminum foil. Two brands, Safeway and Reynolds Wrap, were easily obtainable. An evaluation of the gamma ray spectrum obtained after similar irradiations indicated no significant difference between the two types of foil. Indeed, the only real difference was about twenty cents in price.

The two possible photoreactions of aluminum are listed below.

Target (abundance)	Photo reaction E_T Mev	Residual Nucleus 1/2 Life	Principal Gamma Rays Energy Mev	Percent
13 Al27	He3	Na24	1.368	99.0
100.0	23.71	15.0h	2.754	99.0
	2p	Na25	0.98	15.0
	22.42	59s	0.58	14.0
			0.40	14.0
			1.61	6.0

To use the foil as a flux monitor, the sample vials are wrapped with a sheet of aluminum foil. At a suitable time (around 4-5 hours) after the irradiation, the number of

counts in the 1.36 Mev peak due to Na24 are recorded. The activity at the end of the irradiation is then calculated by the following expression.

$$(1) \quad A(o) = \frac{A(t)e^{\lambda t}}{\varepsilon} \quad \text{dps}$$

where $A(o)$ = activity at the end of the irradiation
$A(t)$ = activity at time t
λ = decay constant
ε = total detector efficiency

The flux is then calculated by

$$(2) \quad \Phi = \frac{A(o)}{N_o \sigma (1-e^{-\lambda T}) f} \quad \frac{\text{photons}}{\text{cm}^2 \cdot \text{sec}}$$

where N_o = number of target atoms
σ = reaction cross section
$1-e^{-\lambda T}$ = saturation factor
T = time of irradiation
f = isotopic abundance

It is important to realize that the flux given by equation (2) is not the actual flux present in the sample. This is because both the reaction cross section and the photon flux are functions of the photon energy. Strictly speaking, the quantity which should be solved for in equation (2) is the product $\sigma\Phi$. To be correct, the production rate for a photonuclear reaction must be calculated by summing the product of the cross section and the photon flux in an energy increment over the energy range of interest [Ref. 16: p. 426]. However, as a quick check on the homogeneity of an irradiation, equation (2) is still useful. As an example, consider two separate irradiations of a sample. Using the

procedure described above, ϕ_1 and ϕ_2 are calculated for the two aluminum foils. The ratio of ϕ_1/ϕ_2 is given by

$$(3)\ \frac{\phi_1}{\phi_2} = \frac{A_1(o)\ No_2}{A_2(o)\ No_1}$$

Equation (3) is useful as an order of magnitude check for an analysis. In one of the experiments for oil, ϕ_1 was calculated as 4.4×10^2 photons/cm^2/sec. ϕ_2 was calculated as 3.3×10^8 photons/cm^2/sec. The ratio was thus 1.33 indicating a 33% difference in flux. This variance of flux is common in beam experiments and is another reason the comparative assay is favored over separate irradiations.

Another use for the aluminum foil is as a check for thermal neutron interfering reactions. For example, the aluminum foil from a one-half hour irradiation of a sample with 100 Mev bremsstrahlung radiation was counted with the NaI(Tl) detector. The following photopeaks were observed.

Peak Energy (Mev)	Production Mechanism
0.511	Annihilation Peak
0.848, 1.015	Mg26(n,γ) Mg27
1.35, 2.74	Al27(γ,He^3) Na24

Mg27 is produced in the following manner.

Primary reaction Al27(γ,p) Mg26.
Subsequent reaction Mg26(n,γ) Mg27.

The implication of the above is that for major and perhaps minor constituents, products other than those

produced by photoreactions may be encountered in a spectrum. This, of course, complicates the analysis.

2. Charcoal Residue

A 25 milliliter sample of charcoal residue was collected from the remains of a barbecue. The sample was irradiated for 10 minutes using a 100 Mev electron beam and a 5.3mm lead convertor. Gamma ray spectrums were recorded over a 45 day period at various times after the irradiation. The nuclear reactions observed are listed in Table IV. Some insight into the thought processes involved in activation analysis will be provided by a discussion of how the elements in the matrix were deduced from the experimental data.

The first clue as to what elements are in a sample comes from either previous knowledge of the sample or a literature search. For charcoal residue it can be assumed that the matrix is similar to fly ash. Table V lists concentrations of various elements found in fly ash. It can be seen that the fly ash matrix is composed mainly of iron, silicon, calcium, potassium and magnesium. Thus, it can be expected that these elements will be found in the charcoal residue. Assuming these elements are in the charcoal residue the probable reactions are listed. (Toms [Ref. 9, 10] is useful for this task.) The things to consider in deciding which reactions are probable include the following: isotopic abundance, cross sections, half-lives of products,

Table IV. Reactions Observed in the Photoactivation of Charcoal Residue

Target Nucleus (abundance)	Photo-reaction	Residual Nucleus 1/2 Life	Principal Gamma Rays Energy (Mev)	Principal Gamma Rays Percent
19K39 93.08	(γ,n)	K38 7.7m	2.170	100.0
20Ca40 96.97	(γ,np)	K38 7.7m	2.170	100.0
20Ca44 2.06	(γ,p)	K43 22.4h	0.374 0.619 1.02	84.7 82.4 2.0
20Ca48 0.18	(γ,n)	Ca47 4.5d	1.297	75.0
20Ca47	beta minus decay to	Sc47 3.4d	0.159	70.0
12Mg25 10.00	(γ,p)	Na24 15.0h	1.368 2.754	99.0 99.0
12Mg26 11.01	(γ,np)	Na24 15.0h	1.368 2.754	99.0 99.0
12Mg24 78.99	(γ,2n)	Mg22 4.0S	no gamma rays observed	
Mg22	beta plus decay to	Na22 2.6y	0.511 1.275	180.0 100.0
26Fe56 91.66	(γ,np)	Mn54 312.5d	0.834	100.0
26Fe57 2.19	(γ,p)	Mn56 2.6h	0.847	99.0
14Si29 4.70	(γ,p)	Al28 2.3m	1.78	100.0
14Si30 3.09	(γ,p)	Al29 6.6m	1.28	93.0

Table V. Trace Element Concentrations in Coal, Fly Ash, and Fuel Oil [Ref. 19: p. 244]

Trace element	Coal, ppm	Fly ash, ppm[b]	Residual fuel oil, ppm
Hg	0.02–2	0.1–<18	0.002–0.4
Be	<0.1–0.4	1–7	0.0005–<0.5
Cd	0.7–<30	2–<100	0.003–1
As	0.25–<100	2.8–<200	0.2–<1
V	5.5–10	180–2000	40–113
Mn	1.9–20	150–500	0.21–1
Ni	4–<40	45–300	20–90
Sb	0.04–<30	5.6–<100	0.003–<0.5
Cr	3.4–<30	80–500	0.7–4
Zn	5–<100	70–1000	0.4–2.0
Cu	<0.4–10	33–300	0.2–1
Pb	1.8–<30	95–440	1–4
Se	0.1–<15	0.77–40	0.02–0.15
B	5–15	190–500	0.002–0.2
F	<2–60	<10–100	0.004[d]
Li	0.3–<300	20–300	0.02–<3
Ag	<0.1–<2	0.04–<3	0.0006–0.1
Sn	0.19–<30	1.9–<100	0.01–5
Fe	1800–8000	5.3%–26%	10–20
Sr	46–160	69–<1000	<0.4–<0.5
Na	100–870	500–6600	<0.4–30
K	20–2200	0.5%–3.1%	0.8–5
Ca	5500–1000	1.3%–5%	7–<400
Si	3000–20000	>10%–20%	8–30
Mg	600–2000	2200–44000	2–3
Ba	<2–500	110–700	0.3–5
P	NA[c]	NA	NA
S	NA	NA	NA

irradiation time, irradiation energy, and counting conditions. In this sense, probably refers to the probability that a gamma ray corresponding to a particular radionuclide will be observed. For example, the (γ,n) reaction of Mg24 produces 12.1 second Mg23 with a gamma ray at 0.439 Mev. While the probability of this reaction occurring is high, the probability of observing the 0.439 Mev gamma ray is small unless the sample is counted immediately after the irradiation.

Once the probable reactions are listed, the sample is irradiated. Gamma ray spectra are then recorded at various times following the irradiation. Gamma ray energies are assigned to each photopeak and if possible half-lives corresponding to a given photopeak are measured. Using the gamma ray energy, the half-life, if measured, and the predicted reactions, the elements in a matrix can be deduced. In the case of the charcoal residue, the 0.347, 0.619 and 1.02 Mev gammas positively identified K43, from which the presence of Ca44 could be deduced. Likewise, the presence of two prominent peaks at 1.37 and 2.75 Mev identified Na24. The most likely reaction producing Na24 is the (γ,p) reaction of Mg25.

Following the above procedure, the majority of the elements in a sample can be easily determined. However, in the case of unexpected gamma rays, a bit of nuclear sleuthing

may be necessary. For instance, in specta taken of the coal residue sample three weeks after the irradiation, the following peaks appeared consistently: 0.511, 0.847, 1.27 and 1.81 Mev. Careful analysis seemed to indicate that the peaks were not decaying, so no half-life information was obtainable except to say that the half-life must be greater than 30 days. Checking a list of possible photoreactions which would produce a gamma ray energy corresponding to any of the observed gamma rays yielded the (γ,np) reaction of Fe26 producing Mn54 with a 312.5 day half-life and a 0.834 gamma ray. The observed 0.847 Mev gamma ray does not quite agree with 0.834 Mev but given the resolution of the NaI(Tl) detector used, a difference of 0.013 Mev is reasonable. However, in a 10 minute irradiation it does not seem plausible that much activity can be expected from a nuclide with a 312.5 day half-life. Nonetheless, it is concluded that the reaction did occur for four reasons. One, the presence of iron in the sample was identified by other reactions. Two, the intensity times abundance for the 0.834 gamma ray is quite high (91.66%). Three, the reaction was observed by Kenneth Murray in a 50 mg sample of Hawaiian pumice with a 27 Mev bremsstrahlung irradiation for 5 hours [Ref. 10: p. 1]. Four, the reaction was observed in an oil sample spiked with 5000 ppm of iron. (see page 83).

The identification of the 0.511, 1.27 and 1.81 Mev gamma rays proved more difficult. First, it was not possible to find a photoreaction which would produce a nuclide with the required gamma rays. A search was then conducted for possible (n,γ) reactions which might have accounted for the observed activity. This effort was futile. Finally, by accident, it was noticed that the gamma ray combination was identical to the decay scheme of Na22. (Note, 1.81 is a sum peak.) Na22 can be produced via the Mg24 (γ,n)Mg23 reaction. Mg23 is not observed because its half-life is 4.0 seconds. However, the decay of Mg23 to Na22 will yield the sought after gamma energies.

The above discussion again points out the degree of complexity which is introduced in a gamma ray spectrum if more than a few nuclides are decaying in a sample. It should be remembered that a proper choice of irradiation time, irradiation energy, and counting schedule can help simplify the analysis.

3. Charcoal

The charcoal sample was obtained by crushing a briquette of Kingsford "Match Light". Enough charcoal was crushed to fill a 25 milliliter polyethylene vial identical to the type used for the charcoal residue sample. The sample was irradiated for 10 minutes using a 70 Mev electron beam and a 5.3mm lead convertor.

Typical elements known to exist in coal are listed in Table V. The major constituent is carbon. Minor elements include iron, potassium, calcium, silicon and magnesium. Thus, the charcoal matrix is very similar to the charcoal residue matrix. Comparing Table IV to Table VI, it can be seen that essentially the same reactions occur in both samples.

Table VI. Reactions Observed in the Photoactivation of Charcoal

Target Nucleus (abundance)	Photo-reaction	Residual Nucleus 1/2 Life	Principal Gamma Rays	
			Energy (Mev)	Percent
6C12 98.89	(γ,n)	Be7 53.3d	0.477	10.3
12Mg25 10.00	(γ,p)	Na24 15.0h	1.368 2.754	99.0 99.0
12Mg25 11.01	(γ,np)	Na24 15.0h	1.368 2.754	99.0 99.0
19K39 93.08	(γ,n)	K38 7.7mm	2.170	100.0
20Ca40 96.97	(γ,np)	K38 7.7mm	2.170	100.0
20Ca44 2.06	(γ,p)	K43 22.4h	0.374 0.619 1.02	84.7 82.4 2.0
20Ca48 0.18	(γ,n)	Ca47 4.5d	1.297	75.0
Ca47	beta minus decay to	Sc47 3.4d	0.159	70.0

An unidentified photopeak in the charcoal spectra is a 0.706 Mev gamma ray. This peak also appears in the oil samples on a regular basis, so it may somehow be associated with the presence of the carbon in the samples. However, no production reaction to account for the peak could be found. A rough half-life is 21 minutes which agrees with the 20.5 minute half-life of C11 produced in the C12 (γ,n) C11 reaction.

4. Potting Soil

A sample of commercial potting soil was analyzed. The interst in this sample was the continued development of techniques which could be used to analyze petroleum samples.

Some information on the composition of the soil matrix was found by reading the label on the package of soil purchased. The contents of the soil included a mixture of sandy loam, forest products, charcoal, perlite, iron and peat moss. The active ingredients were .05% organic nitrogen and .005% thiamin hydrochloride.

An 8.2 gram sample of soil was irradiated for 10 minutes using a 70 Mev electron beam and a 5.3mm lead convertor. The radionuclides observed and their probable mechanism of production are listed in Table VII. The major and minor elements observed were carbon, calcium, magnesium, silicon and iron. Unidentified peaks at 0.703 and 0.913 Mev were also noted.

Table VII. Reactions Observed in the Photoactivation of Potting Soil

Target Nucleus (abundance)	Photo-reaction	Residual Nucleus 1/2 Life	Principal Gamma Rays	
			Energy (Mev)	Percent
14Si29 4.70	(γ,p)	Al28 2.3m	1.78	100.0
14Si30 3.09	(γ,p)	Al29 6.6m	1.28	93.0
6C12 98.89	(γ,n)	Be7 53.3d	0.477	10.3
12Mg25 10.00	(γ,p)	Na24 15.0h	1.368 2.754	99.0 99.0
12Mg26 11.01	(γ,np	Na24 15.0h	1.368 2.754	99.0 99.0
19K39 93.08	(γ,n)	K38 7.7m	2.170	100.0
20Ca40 96.97	(γ,np)	K38 7.7m	2.170	100.0
20Ca44 2.06	(γ,p)	K43 22.4h	0.374 0.619 1.02	84.7 82.4 2.0
20Ca48 0.18	(γ,n)	Ca47 4.5d	1.297	75.0
20Ca47	beta minus decay to	Si47 3.4d	0.159	70.0
26Fe57 2.19	(γ,p)	Mn56 2.6h	0.847	99.0

5. Bismuth Germanate ($Bi_4Ge_3O_{12}$)

A 99.99% pure crystal of BGO was irradiated for 90 seconds with a direct beam of 100 Mev electrons. The beam intensity was measured as 4.8×10^{11} electrons/second.

Table VIII lists the possible photoreactions for BGO. It was assumed that the radionuclides produced would predominately be from (γ,n), (γ,p) reactions. However, all reactions are possible since the irradiating energy will produce bremsstrahlung well above the giant dipole resonance.

Table VIII. Possible Photoreactions with BGO

Target Nucleus (abundance)	Photon reaction	Residual Nucleus Half Life	Principal Gammas Energy (Mev)	Principal Gammas Percent %	Percent x Abundance
8O16 99.8	n	015 124S	0.511	200.0	200.0
32Ge70 20.5	np	Ga68 68.3m	1.078	4.0	0.82
32Ge72 27.4	He3	Zn69 13.8h	0.439	100.0	27.4
	np	Ga70 21.1m	1.040	0.5	0.14
32Ge73 7.8		Zn69m 13.8h	0.439	100.0	7.80
	p	Ga72 14.1h	0.835	83.3	6.50
			2.201	27.3	2.13
			0.630	26.7	2.08
			0.601	8.2	0.64
			1.050	6.9	0.54
			2.490	6.8	0.53

Table VIII contd.

Target Nucleus (abundance)	Photon reaction	Residual Nucleus Half Life	Principal Gammas Energy (Mev)	Principal Gammas Percent %	Percent x Abundance
32Ge74 36.5	∝	Zn69m 13.8h	0.439	100.0	36.5
	np	Ga72 14.1h	0.835	83.3	30.4
			2.201	27.3	9.96
			0.630	26.7	9.74
			0.601	8.2	2.99
			1.050	6.9	2.52
			2.490	6.8	2.48
32Ge74 36.5	p	Ga73 4.9h	0.054	100.0	36.5
			0.295	99.0	36.2
			0.74	6.0	2.19
32Ge76 7.8	T	Ga73 4.9h	0.054	100.0	7.80
			0.295	99.0	7.72
			0.74	6.0	0.47
	n	Ge75 82m	0.2646	10.6	0.83
32Ge70 20.5	T	Ga67 78.2h	0.094	72.12	14.78
			0.296	23.03	4.72
			0.185	21.95	4.50
			0.388	5.74	1.18
			0.091	2.20	0.45
			0.206	1.52	0.31
	n	Ge69 39.2h	1.107	28.10	5.76
			0.573	12.62	2.59
			0.872	9.41	1.93
			1.335	3.05	0.63
			0.320	1.23	0.25
			0.553	0.50	0.10
			0.788	0.35	0.07
			0.237	0.32	0.07
			1.052	0.30	0.06
			1.206	0.26	0.05

Table VIII. contd.

Target Nucleus (abundance)	Photon reaction	Residual Nucleus Half Life	Principal Gammas Energy (Mev)	Principal Gammas Percent %	Percent x Abundance
83Bi209	3n	Bi206	0.803	99.0	99.0
100.0		6.24d	0.880	72.0	72.0
			0.516	46.0	46.0
			1.720	36.0	36.0
			0.538	34.0	34.0
			0.343	26.0	26.0
			0.184	21.0	21.0
			0.895	19.0	19.0
			1.099	13.0	13.0
			0.398	10.0	10.0
			1.019	8.0	8.0
			1.596	8.0	8.0

Table IX is a summary of the photoreactions from Table VIII. The information is arranged to assist in the identification of the origin of the photopeaks observed in the gamma ray spectrum. The last column is five times the half-life of the residual nucleus. This is the time when the radaioactive nucleus no longer contributes significantly to the gamma ray spectrum.

The irradiated crystal was counted at regular intervals for a period of eleven days following the irradiation. Figure 9 is a sample spectrum recorded five hours after the irradiation.

Table IX. Summary of Possible Photoreactions of BGO

Residual Nucleus	Half-Life	Produced From	5 x Half-Life
O15	124S	O16	10.3m
Ga70	21.1m	Ge72	105.5m
Ga68	68.3m	Ge70	5.7h
Ge75	82m	Ge76	6.8h
Ga73	4.9h	Ge74, Ge76	24.5h
Zn69m	13.8h	Ge72, Ge73, Ge74	69h
Ga72	14.1h	Ge73, Ge74	70.5h
Ge69	39.2h	Ge70	196h
Ga67	78.2h	Ge70	391h
Bi206	6.24d	Bi209	31d

Table X. Reactions Observed in the Photoactivation of BGO

Isotope	Production Reaction	Method of Verification
Ga73	Ge74 (γ,p) Ga73	.295 photopeak
Ga72	Ge73 (γ,p) Ga72 and/or Ge74 (γ,np) Ga72	Photopeaks plus half-life of 2.49 Mev gamma
Ge69	Ge70 (γ,n) Ge69	Photopeaks
Bi206	Bi209 (γ,3n) Bi206	Photopeaks plus half-life of 1.72 Mev gamma

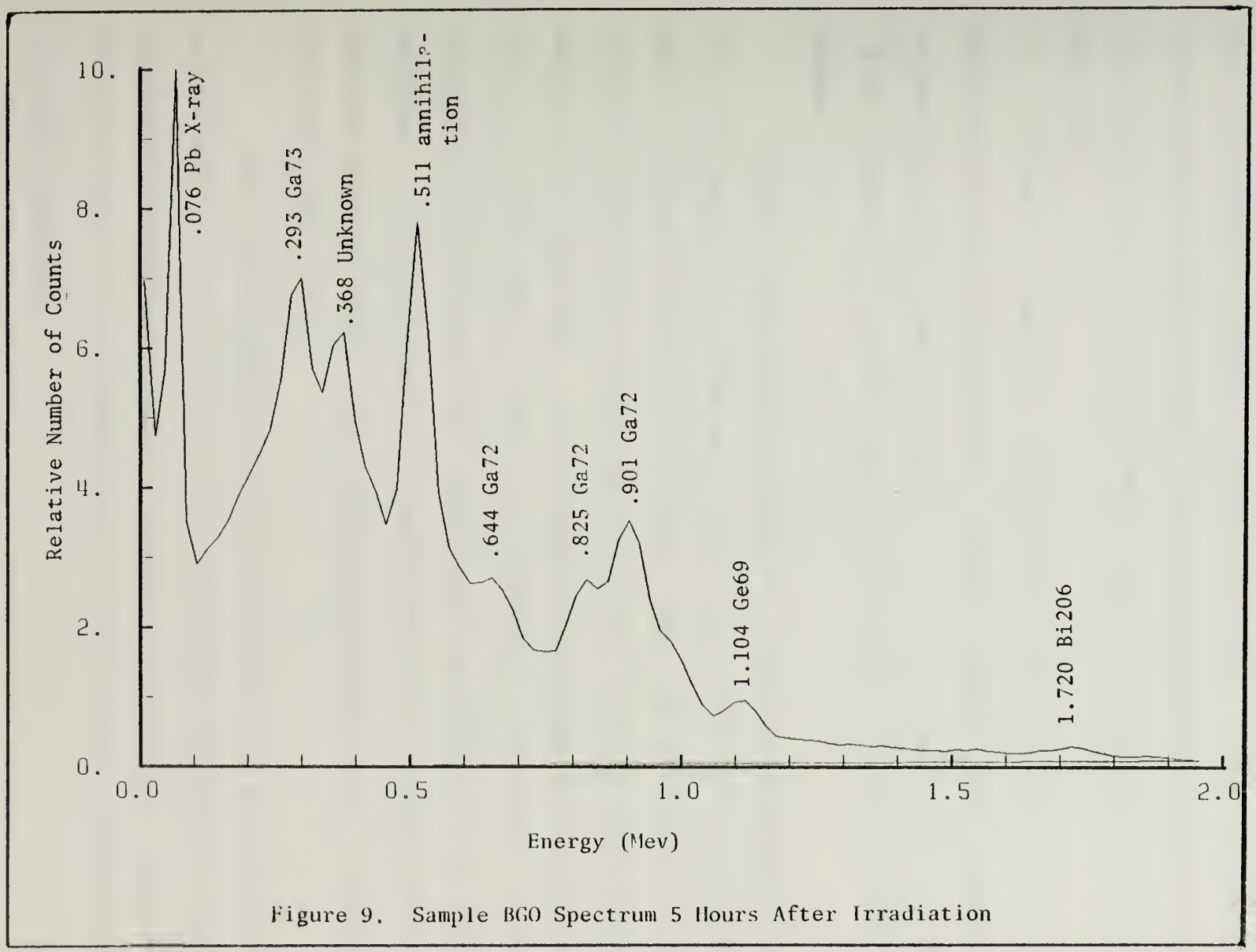

Figure 9. Sample BGO Spectrum 5 Hours After Irradiation

A reaction not predicted as probable, but nonetheless observed, was the (γ,3n) reaction of Bi209. This unexpected reaction is a good example of the complexity which can be introduced into an analysis when higher irradiating energies are used.

There is another interesting way in which the data obtained can be manipulated in order to calculate a nuclear parameter of interest. That is, the cross section for the (γ,3n) reaction of Bi209 can be estimated in the following manner.

First, the photon flux is estimated using equation (2) from page 48 and the activity in the 2.49 Mev photopeak due to the Ge73 (γ,p) Ga72 rection. Next the activity in the 1.72 Mev peak due to Bi206 is measured. Finally, the cross section for the (γ,3n) reaction can be calculated by equation (2), page 48. This technique of finding the Bi209 (γ,3n) cross section will provide a ball park estimate of the cross section. For more precise measurements, monochromatic photons must be used. Such experiments were done by Berman and Fultz [Ref. 25].

The investigation of BGO concludes the preliminary experiments of this thesis. The techniques developed in the analysis of charcoal, charcoal residue, potting soil, and BGO will be used in the following sections to investigate petroleum samples.

D. IPAA - PETROLEUM SAMPLES

1. Background

The determination of trace elements in oil is a major area of interest for the petroleum industry as well as for the U.S. Coast Guard. In the former case, the driving force is mainly economics. The performance of oil driven macahinery, for example, is very sensitive to certain concentrations of trace elements such as vanadium. On the other hand, the U.S. Coast Guard is interested in trace element analysis for its forensic possibilities.

Various analytical techniques have been used to fingerprint oils. These include: IR spectrometry, thin layer chromatography, gas chromatography, mass spectrometry, atomic absorption, non-dispersive x-ray flourescence, neutron activation analysis, and others. To the best of this author's knowledge, no attempts have been made to use photon activation analysis to investigate oils. The possibility of using instrumental photon activation analysis as a rapid, routine method to obtain information about the source of an oil spill was the major impetus for these experiments.

2. Composition of Oil

In photon activation, it is often helpful to have some knowledge of the constituents of a sample which is to be irradiated. Such knowledge would be useful in predicting which nuclear reactions may occur during an irradiation. It

would also help in evaluating the experimental data. Fortunately, petroleum is a much studied matrix.

Oil is a generic term which includes crude oil, gasoline, lubricating oil, naptha, kerosene and fuel oils. Fuel oils have been further classified according to their physical properties into five grades: Nos. 1, 2, 4, 5 and 6. However, no matter what type of oil is studied, all oils are composed primarily of two elements: carbon and hydrogen. Sulfur is also present in varying amounts in all crude oils and petroleum products. Other minor constituents include oxygen and nitrogen compounds. Table XI lists some typical concentrations of the major and minor constituents of various oils. A general classification for concentration ranges is given below.

major element	1.0 to 100.0%
minor element	0.01 to 1.0%
trace element	10^{-4} to 10^{-2}% (1 to 100 ppm)
subtrace element	< 10^{-4}% (< 1 ppm)

Table XI. Major and Minor Constituents of Various Oils [Ref. 18]

	Carbon	Hydrogen	Sulphur	Nitrogen	Oxygen
	Percent				
Crude oil	86.06	13.88	.06	.00	.00
Crude oil	85.05	12.30	1.75	.70	.00
Crude oil	84.00	12.70	.75	1.70	1.20
Gasoline	84.22	15.73	.05	..	..
Lubricating oil	85.12	14.87	.01	..	..
Residual fuel oil	85.70	13.93	.37	..	..
Residual fuel oil	87.10	12.43	.47	..	..
Residual fuel oil	86.40	12.38	1.22	..	..

Trace elements which have been identified in oil include: Na, Mg, Al, Si, P, S, Cl, K, Ca, Ti, V, Cr, Mn, Fe, Co, Ni, Cu, Zn, Ga, As, Br, Sr, Mo, Ag, In, Sn, I, Ba, La, Dy, Au, Pb and Bi. Some of these trace elements are more common than others. For example, Guinn and co-workers analyzed 272 samples of oil using neutron activation analysis [Ref. 17]. While most of the above elements were found in one sample or another, 16 elements were observed on a regular basis in most of the samples. Table XII lists these elements and their frequency of occurence.

Table XII. Trace Elements Found Most Frequently in Oil [Ref. 17: p. 32]

Element	Frequency of Occurence - %
Na	99.6
Br	99.3
Cl	99.3
V	91.2
S	90.8
Mn	89.2
Al	83.7
I	58.5
As	45.2
Ba	44.1
Ni	41.1
Ga	34.1
Dy	34.0
Zn	33.0
Co	18.1
In	15.0

It should be remembered that the trace elements found in oils are strongly dependent on the history of the oil.

That is to say, the trace elements in oil may not be an intrinsic property of the oil. Rather, weathering processes such as an oil coming into contact with salt water or sand, biological attack, or exposure to the sun may drastically alter the trace element composition of the oil. In addition, oil inside a holding tank may pick up foreign contaminants such as tank scale (rust) or dirt. The implications of the above facts of life are that careful attention must be given to how samples are collected and even more careful attention to how the results of an analysis are interpreted.

3. Oil Samples from the Coast Guard Research and Development Center

Five oil samples coded as P-3, P-7, P-11, P-21 and P-42 were analyzed.

a. P-3 Versus P-42

Samples of P-3 and P-42 were irradiated separately for 30 minutes using bremsstrahlung from a 100 Mev electron beam and a 5.3mm lead convertor. Each sample was counted for 30 minutes at nine hours and at twenty-four hours after the irradiation. After a background spectrum was subtracted, the peaks observed from both oils were identical. At the nine hour mark, an intense peak at .477 Mev, a prominent peak at 1.38 Mev and weak peaks at .387, .628 and 1.94 Mev were observed. The same peaks were present after twenty-four hours although with less intensity. The origins

of these peaks are listed below. When the spectrua of P-3 and P-42 were overlapped, there was no significant difference between the two spectra. Based on this limited analysis, it is concluded that the two oil samples are from the same source.

The peaks observed in samples P-3 and P-24 are believed to be from the following reactions.

Peak Energy (Mev)	Source
0.477	$Cl2(\gamma,\alpha n)Be7$
0.387 0.628	$Ca44(\gamma,p)K43$
1.38	$Mg25(\gamma,p)Na24$
1.94	Sum peak 0.477 + 1.38

b. P-7 Versus P-21

Samples P-7 and P-21 were irradiated separately for 30 minutes each using bremsstrahlung from a 62 Mev electron beam and a 5.3mm lead convertor. The average flux for both samples was on the order of 3.5×10^{-8} photons/cm^2/sec.

By increasing the distance of the source to the detector and by using a one-half inch lucite disk to attenuate positrons, it was possible to count both samples one hour after the irradiation. In a fifteen minute count the following peaks were observed in the P-21 spectrum.

Peak Energy (Mev)	Source
0.511	Annihilation peak
1.175, 2.177, 3.376	Cl35(γ,n)Cl34mm
1.47	K40 (background)
1.67	sumpeak .511 + 1.175

No peaks (other than the .511 Mev peak) were observable in the P-7 spectrum one hour after the irradiation.

Additional gamma ray spectrua for both samples were recorded at 2, 3, 4, 5 and 10 hours after irradiation. Other peaks appearing in the P-21 spectrums were:

Peak Energy (Mev)	Source
0.143	Cl35(γ,n)Cl34mm
0.385, 0.619	Ca44(γ,p)K43
1.38, 2.75	Mg25(γ,p) Na24
0.708	Unknown

Peaks observed in the P-7 spectra were:

Peak Energy (Mev)	Source
0.184	Unknown
0.511	Annihilation Peak
0.710	Unknown
1.38	Mg25(γ,p) Na24

Comparing P-7 and P-21 it is concluded that they are from different sources. This observation is based on the presence of chlorine and calcium in P-21 but not in P-7.

c. Irradiation of P-11

Sample P-11 was irradiated for 30 minutes using bremsstrahlung from a 70 Mev electron beam and a 5.3mm lead convertor. The flux was estimated as 3×10^8 photons/cm^2/sec. The following peaks were observed.

Peak Energy (Mev)	Source
0.141 2.11	Cl35(γ,n) Cl34mm
0.511	Annihilation peak
1.02	Sum peak .511 + .511
0.703	Unknown

This sample appears to be a different oil than either P-3, P-7, P-21 or P-42. Because of the presence of chlorine, P-11 is different from P-3, P-7 and P-42. Because of the absence of any potassium43 peaks, P-11 is different from P-21. These results are displayed below.

Element \ Oil Sample	P-3	P-7	P-11	P-21	P-42
Ca	x			x	x
Mg	x	x		x	x
Cl			x	x	

Conclusions: P-3 = P-42
P-7 ≠ P-11 ≠ P-21 ≠ P-3 or P-42

d. Discussion of Results

After the samples were analyzed, information was obtained on the history of the oils. It was learned that samples P-3 and P-42 were indeed identical. Furthermore, samples P-7 and P-11 were from the same drilling platform but were collected one month apart. Finally, sample P-21 was from the same general area as samples P-7 and P-11 but was obtained from a different platform.

Considering this a priori knowledge, the experimental results, showing samples P-7, P-11, and P-21 are from different sources, are reasonable. Although these results were based only on an analysis of the minor constituents in the oils, the results demonstrate the feasibility of using photon activation analysis to fingerprint oils.

4. Oil Samples from the Coast Guard Central Oil Identification Laboratory

Seven samples consisting of 2 crude oils, 2 lube oils, 1 fuel oil #5, 1 fuel oil #6 and 1 bunker "C" fuel oil were investigated. The irradiation time varied between 10 minutes and 30 minutes. The electron beam energy was either 70 or 100 Mev and the lead convertor was used for all irradiations.

The results of these irradiations are summed up with one word--uneventful. Except for one lube oil sample where the concentration of calcium was determined, the only other

significant activity was due to the presence of carbon in the oils. These results are not too surprising considering the composition of oil as explained previously and considering the average beam current for the irradiations was less than 1 uA.

Table V lists trace element concentration ranges for a sample of fuel oil #6. Although the listed concentrations are not necessarily representative of the trace element content of fuel oils from different sources, the table does imply that calcium may be present in a fuel oil at the minor element level. This was indeed the case for one of the lube oil samples.

It was mentioned that the history of an oil may drastically alter the concentration of elements found in oils. Therefore, it is not uncommon to find certain elements in minor amounts in oils. A good example would be a high concentration of sodium and chlorine found in an oil spill sample collected from the open ocean.

5. Automotive, Used Engine Oil

A sample of used engine oil was irradiated for 10 minutes using a 100 Mev electron beam and a 5.3mm lead convertor. Gamma ray spectra were collected over an eleven day period. The gamma rays observed and the probable nuclides producing the gamma ray are listed in Table XIII. Overlapping gamma rays made it difficult to measure a half-

life for most of the photopeaks. The half-life for the 0.278 Mev gamma ray was measured as approximately 34 hours. Analysis of the 0.364 Mev photopeak was complicated by an uneven compton distribution from the 0.477 Mev photopeak. A rough calculation yielded a half-life of about 60 hours for the 0.364 Mev photopeak. A similar observation of an unknown gamma ray with an energy of 0.362 Mev and a half-life of 60 hours was reported by Aras and co-workers in their analysis of atmospheric particulate material [Ref. 15: p. 1485].

Table XIII. Gamma Rays Observed in the Photoactivation of a Sample of Used Engine Oil

Gamma Ray Energy (Mev)	Probable Gamma Source	Target Nucleus
.036	Unknown	
.078	Pb X-ray	
.155	Hg199	Pb204
.185	Unknown	
.278	Ba133m, Ba135m	Ba134,135,136, 137
.364	Unknown	
.477	Be7	Cl2
.511	Annihilation	
.620	Unknown	
.833	Cs135m	Ba137, 138
.920	Unknown	
.960	Pb202m	Pb204
1.37	Na24	Mg25, 26
2.74	Na24	Mg25, 26

6. Determination of Calcium in an Oil

Using the methods explained in the theory sections, the concentration of calcium in a sample of marine lube oil

was determined. In particular, a comparative assay was performed using a lube oil sample and an oil standard spiked at 5000 ppm calcium.

Both the sample and standard were irradiated simultaneously for one-half hour using a 70 Mev electron beam and a 5.3mm lead convertor. The irradiation and counting geometries for the sample and standard were identical. The 0.619 Mev photopeak from the Ca44(γ,p)K43 reaction was analyzed because there were no higher energy photopeaks appearing in the spectrum whose compton distributions would contribute significantly to the observed activity in the 0.619 Mev photopeak.

Spectra used for the calculations were obtained at around nine hours and twenty-five hours after the irradiation. Equation 7 from Chapter II-D is the appropriate equation to use. The results follow.

(Equa. 7) $$\frac{W_x}{W_s} = \frac{A_x(tx)e^{\lambda tx}}{A_s(ts)e^{\lambda ts}}$$

Pertinent Data:

$W_s = 1.70 \times 10^{-2}$ grams
$\lambda = .0309\ hr^{-1}$
s = 3.4467 grams

Run	A_x(cpm)	t_x(hr)	A_s(cpm)	t_s(hr)
1	27.6	9.0	453.1	9.5
2	18.6	25.0	264.2	26.0

Calculations:

Run 1: $W_x = \frac{27.6e^{.0309(9.0)}}{453.1e^{.0309(9.5)}} 1.70 \times 10^{-2}$

$W_x = 1.02 \times 10^{-3}$ grams

$C_x = \frac{W_x}{S} \times 10^6 = 296$ ppm

or $C_x = \frac{W_x}{S} \times 10^2 = .029\%$

Run 2: $W_x = \frac{18.6\ e^{.0309(25.0)}}{264.2\ e^{.0309(26.0)}} 1.70 \times 10^{-2}$

$W_x = 1.16 \times 10^{-3}$ grams

$C_x = W_x/S \times 10^6 = 336$ ppm

or $C_x = W_x/S \times 10^2 = .033\%$

Error Analysis:

The standard deviation of the counting rate is $\pm \sqrt{C}/t$ where C is the number of counts in a time interval t. It is assumed that the half-life of K43 is accurately known as 22.4 hours. The times of measurements were with ± 1 minute. Compared to the length of times when the spectra were recorded (9, 9.5, 25 and 26 hours), an insignificant error is introduced by a ±1 minute difference. The weights of the sample and standard were precisely measured to within ±.0001 gram. This precision also contributes an insignificant error to the analysis. Therefore the largest contribution to the error is in the measurement of the radioactivity.

For run 1 the counting time was 30 minutes. For run 2, it was one hour. The counting rates and their standard deviation are then,

Run	A_x (cpm)	A_s (cpm)
1	27.6 ± 1.0	453.1 ± 3.9
2	18.6 ± 0.6	264.2 ± 2.1

The propagation of errors of values that are multiplied or divided is related to fractional errors of the respective values. In general, for the relationship

$$(6\text{-}1) \quad W = \frac{XY}{Z}$$

the standard deviation of W is

$$(6\text{-}2) \quad \frac{\sigma W}{W} = \pm \left[\left(\frac{\sigma X}{X}\right)^2 + \left(\frac{\sigma Y}{Y}\right)^2 + \left(\frac{\sigma Z}{Z}\right)^2 \right]^{1/2}$$

In particular, for equation 7, the standard deviations of W_x is

$$(6\text{-}3) \quad \sigma(W_x) = \pm \frac{A_x(t_x)e^{\lambda tx}}{A_s(t_s)e^{\lambda ts}} W_s \left[\left(\frac{\sigma(A_x)}{A_x}\right)^2 + \left(\frac{\sigma(A_s)}{A_s}\right)^2 \right]^{1/2}$$

When the appropriate numbers are inserted into equation (6-3), the final results for the concentration of calcium in the sample oil are:

Run 1 Concentration of Calcium = 296 ± 37 ppm
Run 2 Concentration of Calcium = 336 ± 38 ppm

The average of these two values is 316 ± 26 ppm. The overall error is then about ± 8% for the measurement.

E. MISCELLANEOUS EXPERIMENTS

1. Spatial Variance of the Photon Flux

An experiment was conducted in order to obtain some information on the spatial distribution of the photon flux. Figure 10 shows the experimental set up.

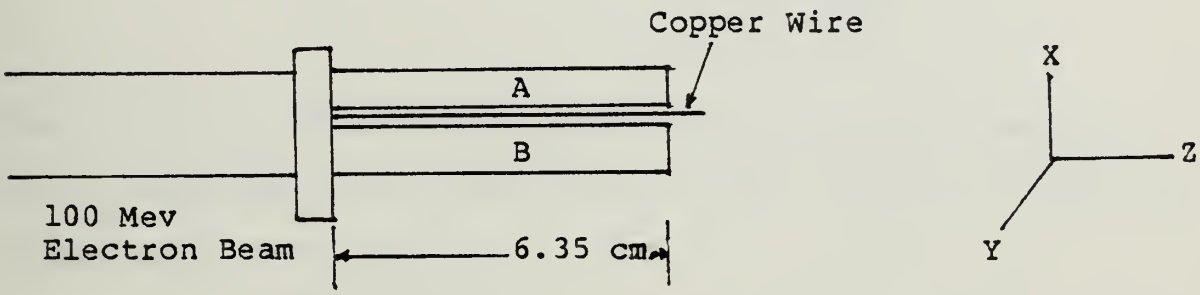

Figure 10. Top View of Experimental Set Up for Flux Experiment

The two targets were glass vials one-half full of oil. Each target was wrapped in a sheet of aluminum foil. A thin copper wire was placed between the two samples. The transverse variance (i.e., x-direction) of the flux was first investigated by doing a gross count of aluminum foils A and B. Using the procedures as explained in Section II-C-1, the average value of the flux for foil A was 2.27×10^8 photons/cm^2/sec. For foil B the flux was 0.27×10^8 photons/cm^2/sec. This large difference in average flux is attributed to misalignment of the targets.

The Z-dependence of the photon flux was determined by cutting foil A into six sections. Each section was about 1

cm long. The sections were then counted individually and the flux determined. The results were:

Section	Flux (photons/cm^2/sec)
1	6.58×10^8
2	3.33×10^8
3	3.66×10^8
4	2.73×10^8
5	2.41×10^8
6	3.31×10^8

When the results are normalized to the flux for section 1, the Z-dependence of the flux is given by the following histogram.

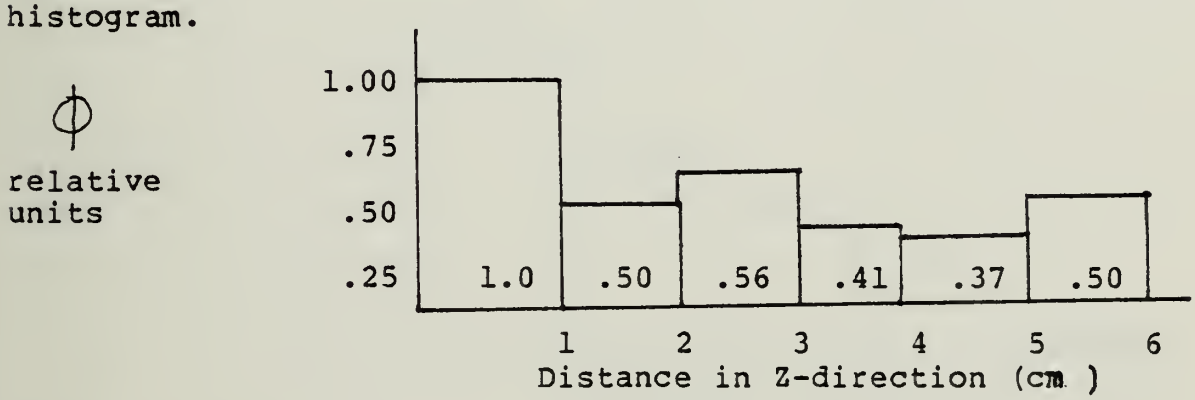

One explanation for the above profile is that the target was completely wrapped with aluminum foil. Therefore, the end sections expose more surface area to the photon flux than the foil on the sides.

As a check on the observed flux profile above, a similar calculation was done using the copper wire. The reaction used was the Cu65(γ,n)Cu64 reaction. The half-life of Cu64 is 12.25 hours and it decays by positron emission and electron capture. Thirty-eight percent of the time a 0.511

gamma ray is emitted. The 0.511 gamma ray was used for calculations. The results were:

Section	Flux (photons/cm^2/sec)
1	3.54×10^9
2	2.21×10^9
3	1.21×10^9
4	$.60 \times 10^9$
5	$.32 \times 10^9$

When these results are normalized, the flux profile is given by:

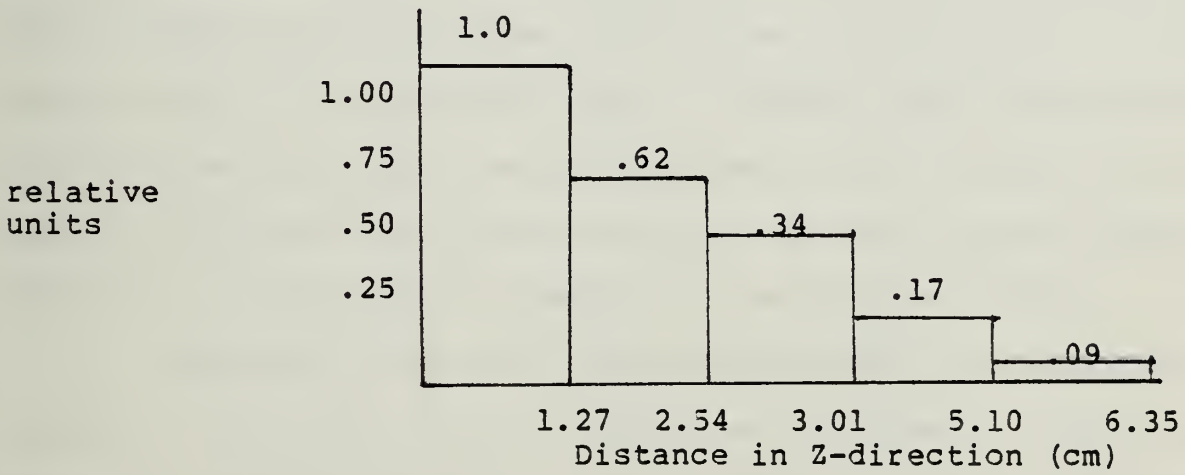

This is a different flux profile than that calculated using the aluminum foil. This is not surprising since only relative calculations were done rather than absolute calculations. For example, no nuclear data for the (γ, He^3) cross section for the aluminum calculation was available. A value of 1 millibarn was used. Assuming accurate values are known for all variables in the calculation (i.e., cross sections,

detector efficiencies, decay schemes, etc.), it would be possible to do an absolute determination of the flux.

The bottom line of this experiment is that it is very difficult to reproduce the same photon flux in different runs of an experiment. Therefore, as mentioned previously, the comparative technique is most often used in activation analysis.

2. IPAA of Oils Spiked With Calcium and Iron

A sample of oil containing 5000 ppm iron and a sample of oil containing 5000 ppm calcium were irradiated. The purpose of the irradiation was to observe the gamma rays emitted due to a known amount of element in a sample. The spectra obtained would then be useful in identifying gamma rays due to either iron or calcium in an unknown sample.

Table XIV lists the reactions observed in the calcium sample. Table XV lists the reactions observed in the iron sample. In both samples a strong peak at 0.710 Mev was observed. In neither case could this peak be attributed to the iron or calcium activity.

Table XIV. Reactions Observed in the Photoactivation of an Oil Sample Spiked with 5000 ppm Calcium

Target Nucleus (abundance)	Photo-reaction	Residual Nucleus 1/2 Life	Principal Gamma Rays	
			Energy (Mev)	Percent
20Ca43 0.145	(γ,2p)	Ar41 1.8h	1.293	99.2
	(γ,p)	K42 12.4h	1.528	18.0
20Ca44 2.06	(γ,He3)	Ar41 1.8h	1.293	99.2
	(γ,np)	K42 12.4h	1.528	18.0
	(γ,p)	K43 22.4h	0.374	84.7
			0.619	82.4
			1.02	2.0
20Ca48 0.18	(γ,n)	Ca47 4.5d	1.297	75.0
20Ca47	beta minus decay to	Sc47 3.4d	0.159	70.0

Table XV. Reactions Observed in the Photoactivation of an Oil Sample Spiked with 5000 ppm Iron

Target Nucleus (abundance)	Photo-reaction	Residual Nucleus 1/2 Life	Principal Gamma Rays	
			Energy (Mev)	Percent
26Fe54 5.82	(γ,2n)	Fe52 8.2h	0.165	100.0
26Fe56 91.66	(γ,np)	Mn54 312.5d	0.834	100.0
26Fe57 2.19	(γ,p)	Mn56 2.6h	0.847 1.811 2.110	99.0 29.0 15.5
26Fe58 0.33	(γ,np)	Mn56 2.6h	0.847 1.811 2.110	99.0 29.0 15.5

IV. SUMMARY AND CONCLUSIONS

The first part of this thesis reviewed the basic principles of photon activation analysis. It was noted that the technique had been used successfully in the investigation of a variety of materials. In the second part of the thesis, experiments with general samples showed that the major and minor elements in a sample could be easily activated. The most common elements observed in biological and environmental samples were carbon, silicon, calcium, potassium, magnesium and iron.

After investigating the general samples, various samples of oils were analyzed. Even though no trace elements were observed, it was still possible to make tentative comparisons of oils based on the minor constituents. A quantitative analysis for calcium showed that it was possible to detect elements at a concentration of .03% (300 ppm).

An interesting peak appeared in many spectra at 0.710 Mev. It is believed that this peak is a sum peak due to the intense activity of the 0.511 Mev peak. For example, if the 0.511 Mev peak and its backscatter peak are counted simultaneously, a peak would appear around 0.7 Mev. The half-life associated with the 0.710 Mev peak, measured as 21 minutes, is further evidence for this hypothesis. It is known

that the 0.511 peak is mainly due to carbon 11 which has a half-life of 20.5 minutes.

A number of conclusions can be stated based on the experimental results. First, even with the low beam current of the LINAC, it is possible to determine major and minor elements in a matrix. A lower limit of detection for most elements is estimated as 100 ppm. Since the range of trace elements is 1 to 100 ppm, higher beam currents are required for trace element analysis. In addition, if a complex matrix such as oil is to be analyzed, many gamma rays can be expected when the sample is counted. Therefore, to avoid overlapping gamma rays, high resolution is important and hence a Ge(Li) detector would be required for any quantitative results.

A second conclusion of this thesis is that it would be beneficial to continue to investigate oil using photon activation analysis. One reason to continue is purely academic. That is, photon activation is a highly sensitive technique which has not been used previously to fingerprint oil spills. The possibility of identifying new elements not previously reported in oils is in itself sufficient reason for further analysis. Perhaps a more practical reason is a recent oil spill case which occurred in the 13th Coast Guard District. In that incident, samples were collected from the spill and suspect vessels and a positive match was made by

the Coast Guard's Central Oil Identification Laboratory. The methods used included infra-red spectrometry, gas chromatography, thin layer chromatography, and uv flourescence. Owners of the suspect vessel also commissioned an analysis of the oil samples using neutron activation analysis. The interpretation of the results of the neutron activation analysis apparently did not agree with the Coast Guard's tests. Armed with this knowledge, there is the possibility that the suspect vessel's owners may challenge the validity of the Coast Guard tests. Even though the Coast Guard tests have been upheld by the courts, the fact that activation analysis is being considered as a technique to perhaps discredit the present tests is reason for concern. To anticipate any problems in this area, it is recommended that the Coast Guard consider activation analysis as an additional technique of analyzing oils. For example, in oil spill cases where large amounts of money are involved for cleanup and fines, it may be wise to contract for an activation analysis. Towards this end, it would also be helpful to have more than one Coast Guard officer familiar with activation analysis procedures. One way to do this would be to collaborate with the LINAC branch of the National Bureau of Standards. One or two weeks at NBS would be sufficient time to generate enough data for weeks of analysis. The study could easily be developed into an

interdisciplinary thesis project, which could involve students from the physics, computer science and operations research curricula. What would be needed to initiate such a project would be the sponsorship of an appropriate command such as COIL.

As the first step of any possible further work with oil and photon activation analysis, Appendix A is a theoretical analysis of oil using a 125uA beam current and a 60 cm^3 Ge(Li) detector.

The final conclusion of this thesis is that the analysis of oil for trace elements using the Naval Postgraduate School's LINAC is not feasible. However, elements in concentrations down to .01% (100 ppm) may be detected. One possible way to observe elements in oil other than carbon is to burn the oil prior to irradiation. This will eliminate the carbon interference and concentrate the trace elements in the remaining ash. This ash almost always contains amounts of aluminum, calcium, iron, magnesium, nickle, sodium, silicon and vanadium ranging from 0.015% to 0.05% of the ash [Ref. 18: p. 94]. The problem with this method is that the maximum amount of ash in oil is about 0.2%. It would therefore take 500 grams of oil to produce a 1 gram sample of ash.

APPENDIX A

A THEORETICAL ANALYSIS OF A FUEL OIL USING PHOTON ACTIVATION ANALYSIS

Trace element analysis is not possible with the NPGS linear accelerator. Therefore, a hypothetical experiment will be described which will use photon activation analysis to analyze an oil sample. The sample to be studied is a number 6 residual fuel oil. The concentration of 26 trace elements in this oil were determined in an interlaboratory comparison study [Ref. 19: p. 244]. These elements and their concentrations are listed in Table A-1. The concentration values underlined were determined by neutron activation analysis.

The experiment to be discussed can be considered a "what if" experiment. That is to say, "What if it is assumed that the known trace element concentrations in an oil sample are in fact unknown. What trace elements could then be detected in a photon activation analysis?" A convenient analysis for this purpose would be one similar to the experiment done by Chattopadhyay and Jervis in their photon activation analysis of market-garden soils [Ref. 12]. They irradiated a one gram sample of soil for a standard irradiation time of one hour. The electron beam energy varied from 8 to 44 Mev. A 3 mm thick, water-cooled tungsten convertor provided an average

flux of 2×10^{13} photons/cm^2/sec. The sample was placed 1 cm away from the rear face of the convertor. The typical average beam current measured on the convertor ranged from 35 to 190 uA. Samples were allowed to "cool" for one hour after the irradiation, then the gamma rays were observed with a 60 cm^3 Ge(Li) detector coupled with a 4096 channel multi-channel analyzer. The FWHM of the detector was 1.9 KeV at the 1.332 Mev photopeak of Co60. The efficiency of the detector was measured as 6.7% with respect to a standard NaI(Tl) detector.

This analysis of the fuel oil sample will assume all the conditions above except only one irradiation energy will be used. The energy chosen is 25 Mev implying a beam current of 125 uA. The reason for this choice is that Chattopadhyay and Jervis feel that a lower electron energy and a higher beam current are sufficient to estimate a number of elements. Using a higher irradiation energy will produce more activity, but it will also enhance interfering reactions.

Table A-2 lists the probable photoreactions expected for the elements in Table A-1. The considerations in deciding which reactions are probable are: (a) The (γ,n), (γ,p) reaction cross sections are about equal up to atomic number 30. Above Z =30 the (γ,n) reaction will predominate. (b) Since the irradiation energy is 25 Mev, reactions having a threshhold energy above 20 Mev are not likely to produce any measurable activity. (c) The irradiation time of one

hour will favor nuclear products with half-lives less than 20 minutes. (d) However, by waiting one hour before counting, any radionuclide with a half-life less than 10 minutes will probably not be detected.

Table A-3 lists the photoreactions of Table A-2 in order of increasing gamma ray energy. Interference-free gamma rays have been identified with an asterisk. Gamma rays falling within ±4 KeV of each other were considered to be mutually interfering under the counting system used in this analysis.

The interference-free gamma rays in Table A-3 can be used to identify an element in the sample. This is done by measuring a half-life corresponding to each photopeak. Using the gamma ray energy and half-life information, a radionuclide can be associated with each photopeak. The target nucleus and therefore an element in the oil sample can then be deduced. A summary of the elements which can be determined in this manner is listed below. The number in parenthesis is the number of interference-free gamma rays associated with each element.

Elements Which Can be Detected in Oil

(Based on interference-free gammas only)

Ag(4)	As(2)	V (2)	Ca(1)
Zn(3)	Sb(2)	Mg(2)	Ni(1)
Cd(3)	Se(2)	Mn(1)	Cr(1)
Fe(3)	Cu(2)	Hg(1)	Pb(1)

For some of the elements above which yield only one interference-free gamma ray, it is possible to take advantage of different decay rates to obtain additional interference-free gammas. For instance, if the sample is counted 3 days after the irradiation, the 0.065 Mev gamma of Sn119m will be free from any interference from shorter lived isotopes. Another example is the determination of lead. The photopeaks of Zn63 and Pb204m overlap at 0.961 Mev. However, the half-lives of Zn63 and Pb204m are 38 minutes and 3.6 hours respectively. Thus, by counting the sample at around 5 hours after the irradiation, the activity in the 0.961 Mev peak will be due to lead alone. Finally, the 0.374 Mev peak of K43 becomes interference-free if one counts the sample after the activity of Hg199m decays to an insignificant level.

A factor not considered in the above discussion is the relative abundance of the trace elements in the oil sample. This was because the assumption was made that the trace elements in the oil were unknown. However, if the concentration of an element is known, the question must be asked is it within the detection limits of the analysis. The detection limits for this analysis were assumed to be identical to the detection limits determined by Chattopahyay and Jervis. This assumption is not totally valid because detection limits must be restricted to a particular matrix studied and the concentrations of interfering elements in

that matrix. However, since the experimental conditions assumed for the oil sample were identical to the conditions used to analyze the soil sample, it is reasonable to use the same detection limits for both samples. When these detection limits are applied to the oil analysis, it is found that manganese, selinium, silver, antimony and mercury cannot be detected. The lack of gamma rays due to these elements does, however, allow the presence of barium to be determined. The list of elements which can then be determined in the oil sample becomes: Zn, Cd, Fe, As, Cu, V, Mg, Sn, Ca, Ni, Cr, Pb and Ba. It is interesting to compare the above list to a list of the elements determined by neutron activation analysis. Elements which can be determined by either method include: Ca, V, Cr, Fe, Ni, Zn and As. Elements which can be determined by NAA but not PAA include: Sb, Hg, Ag, Se, Mn and Na. Finally, elements detectable by PAA but not NAA include: Mg, Cu, Cd, Sn, Ba and Pb. In both cases 13 elements are detectable. However, the use of PAA allows different elements to be determined than those determined with NAA and vice versa. This comparison, of course, only applies to this particular example. Nonetheless, the general conclusion that PAA and NAA will produce different nuclides is valid.

Another point to consider in this analysis is the presence of trace elements in the oil sample other than the

elements listed in Table A-1. For example, Al, Cl, Co, Ga, Br, In, I and Dy are also commonly found in oil. (See Table XII). It is not known whether or not these elements were detected in the oil sample reported in Reference 19. For the purpose of this analysis it was assumed that they were not present in the oil.

The last comment concerning this study is that for the same oil sample, a different set of experimental conditions will yield different results. Therefore, by varying the irradiating energy, the beam current, or the irradiation time, certain reactions can be enhanced and other reactions can be diminished or eliminated. This flexibility of optimizing certain reactions is one of the major advantages of photon activation analysis.

Table A-1. Trace Element Concentrations of a Residual Fuel Oil Number 6 [Ref. 19: p. 244]

Elements	Concentration (ppm)
Li	3
Be	0.5
B	0.2
F	0.004
Na	7.7
Mg	3
Si	30
K	5
Ca	400
V	113
Cr	1
Mn	1
Fe	20
Ni	62
Cu	1
Zn	1.4
As	0.35
Se	0.15
Sr	0.5
Ag	0.02
Cd	1
Sn	5
Sb	0.01
Ba	5
Hg	0.01
Pb	4

Table A-2. Probable Photoreactions for Sample Fuel Oil

Target Nucleus (abundance)	Photo-reaction (E_t)	Residual Nucleus 1/2 Life	Principal Gammas Energy (Mev)	Principal Gammas Intensity Percent	Intensity times Abundance
6C12	n	C11	0.511	200.0	199.0
98.89	18.7	20.5m	(annihilation peak)		
12Mg25	p	Na24	1.368	99.0	9.9
10.0	12.1	15.0h	2.754	99.0	9.9
20Ca44	p	K43	0.374	84.7	1.8
2.06	12.2	22.4h	0.619	82.4	1.7
20Ca48	n	Ca47	1.297	75.0	0.1
0.18	9.9	4.5d			
		B^- to Sc47 3.4d	0.159	70.0	0.1
23V50	2n	V48	0.983	100.0	0.2
0.24	20.9	16.1d	1.31	97.0	0.2
24Cr50	n	Cr49	0.091	30.0	1.3
4.35	12.9	41.9m	0.062	15.0	0.7
			0.153	14.0	0.6
24Cr52	n	Cr51	0.320	9.9	8.3
83.79	12.0	27.8d			
25Mn55	n	Mn54	0.834	100.0	100.0
100.0	10.2	312.5d			
26Fe57	p	Mn56	0.847	99.0	2.2
2.19	10.6	2.6h	1.811	29.0	0.6
			2.110	15.5	0.3
28Ni58	n	Ni57	0.127	14.0	9.5
67.77	12.1	36h	1.378	86.0	58.2
			1.919	14.0	9.5
28Ni62	p	Co61	0.067	100.0	3.7
3.66	11.1	1.7h			

Table A-2 Contd.

Target Nucleus (abundance)	Photo-reaction (E_t)	Residual Nucleus 1/2 Life	Principal Gammas Energy (Mev)	Principal Gammas Intensity Percent	Intensity times Abundance
29Cu63	2p	Co61	0.067	100.0	69.2
69.17	17.2	1.7h			
	2n	Cu61	0.284	12.0	8.3
	19.7	3.4h	0.655	11.0	7.6
			0.674	4.0	2.8
			0.38	2.5	1.7
			0.58	1.5	1.0
			0.94	1.4	1.0
29Cu65	α	Co61	0.067	100.0	30.8
30.83	6.7	1.7h			
30Zn64	n	Zn63	0.669	8.0	3.9
48.89	11.9	38.4m	0.962	6.0	2.9
30Zn66	n	Zn65	1.115	50.6	14.2
27.81	11.0	244d			
30Zn68	p	Cu67	0.184	40.9	7.6
18.57	10.0	61.6d	0.093	24.5	4.6
30Zn70	n	Zn69m	0.439	100.0	0.6
0.62	9.2	13.8h			
33As75	n	As74	0.596	61.8	61.8
100.0	10.3	17.7d	0.635	14.0	14.0
34Se74	n	Se73	0.359	100.0	0.9
0.87	12.1	7.1h	0.066	100.0	0.9
34Se76	n	Se75	0.265	59.5	5.4
9.02	11.2	120.4d	0.136	57.3	5.2
			0.279	25.2	2.3
			0.121	16.9	1.5
			0.400	12.4	1.1
34Se77	p	As76	0.559	42.0	3.2
7.58	9.6	26.3h			

Table A-2 Contd.

Target Nucleus (abundance)	Photo-reaction (E_t)	Residual Nucleus 1/2 Life	Principal Gammas Energy (Mev)	Principal Gammas Intensity Percent	Intensity times Abundance
34Se82 9.19	n 9.3	Se81m 57m	0.103	100.0	9.2
38Sr86 9.87	n 11.5	Sr85m 70m	0.237 and 0.231	86.0	8.5
38Sr87 7.04	2n 19.9	Sr85m 70m	0.237 and 0.231	86.0	6.1
	γ^1 M4	Sr87m 2.8h	0.388	99.0	7.0
38Sr88 82.53	n 11.1	Sr87m 2.8h	0.388	99.0	81.7
47Ag107 51.82	n 9.5	Ag106m 8.4d	0.511 1.046 0.808 0.717 0.406 0.748 0.616 1.528 + 13 more gammas	89.5 31.1 25.0 23.3 22.3 22.1 20.3 20.2	46.4 16.1 13.0 12.1 11.6 11.5 10.5 10.5
48Cd112 24.07	n 9.4	Cd111m 48.6	0.247 0.150	100.0 100.0	24.1 24.1
48Cd113 12.26	2n 15.9	Cd111m 48.6	0.247 0.150	100.0 100.0	12.3 12.3
48Cd116 7.58	n 8.7	Cd115 53.5h	0.335 0.53	95.0 26.5	7.2 2.0
50Sn118 24.03	n 9.3	Sn117m 14.0d	0.159 0.158	100.0 100.0	24.0 24.0

Table A-2 Contd.

Target Nucleus (abundance)	Photo-reaction (E_t)	Residual Nucleus 1/2 Life	Principal Gammas Energy (Mev)	Principal Gammas Intensity Percent	Intensity times Abundance
50Sn120 32.85	n 9.1	Sn119m 245d	0.065	100.0	32.9
50Sn124 5.94	n 8.5	Sn123m 40m	0.160	100.0	5.9
51Sb121 57.25	n 9.3	Sb120 15.9m	1.171	1.3	0.7
		Sb120 5.8d	1.170 0.200	100.0 100.0	57.3 57.3
51Sb123 42.75	n 8.9	Sb122 2.7d	0.564 0.686	66.3 3.3	28.3 1.4
56Ba134 2.42	n 9.3	Ba133m 38.9h	0.276	100.0	2.4
56Ba135 6.59	γ^1 M4	Ba135m 28.7h	0.268	100.0	6.6
56Ba136 7.81	n 9.2	Ba135m 28.7h	0.268	100.0	7.8
80Hg198 10.02	n 8.6	Hg197 64.1h	0.077	99.9	10.0
80Hg200 23.13	n 8.0	Hg199m 43m	0.375 0.158	100.0 100.0	23.1 23.1
80Hg201 13.22	2n 14.3	Hg199m 43m	0.375 0.158	100.0 100.0	13.2 13.2
82Pb204 1.48	n 8.2	Pb203 52.1h	0.279	99.2	1.5
	2n 15.2	Pb202m 3.6h	0.961 0.422 0.658 0.129	90.0 90.0 78.2 78.2	1.3 1.3 1.2 1.2

Table A-3. Probable Photoreactions for Sample Fuel Oil (Listed in Order of Increasing Gamma Ray Energy)

Energy	Target	Reaction	Product	Half-Life	Intensity times Abundance %
0.062	Cr50	n	Cr49	41.9m	0.7
0.065	Sn120	n	Sn119m	245d	32.9
0.066	Se74	n	Se73	7.1h	0.9
0.067	Ni62	p	Co61	1.7h	3.7
	Cu63	2p	Co61	1.7h	69.2
	Cu65		Co61	1.7h	38.8
0.077*	Hg198	n	Hg197	64.1h	10.0
0.091	Cr50	n	Cr49	41.9m	11.3
0.093	Zn68	p	Cu67	61.6h	4.6
0.103*	Se82	n	Se81m	57m	9.2
0.121	Se76	n	Se75	120d	1.5
0.127	Ni58	n	Ni57	36h	9.5
0.129	Pb204	2n	Pb202m	3.6h	1.2
0.136	Se76	n	Se75	120d	5.2
0.150	Cd112	n	Cd111m	48.6m	24.1
0.153	Cr50	n	Cr49	41.9m	0.6
0.158	Hg200	n	Hg199m	43m	23.1
0.159	Sn118	n	Sn117m	14d	24.0
0.160	Sn124	n	Sn123m	40m	5.9
0.184*	Zn68	p	Cu67	61.6h	7.6
0.200*	Sb121	n	Sb120	5.8d	57.3
0.231	Sr86	n	Sr85m	70m	6.1
	Sr87	2n	Sr85m	70m	6.1
0.237	Sr86	n	Sr85m	70m	6.1
	Sr87	2n	Sr85m	70m	6.1
0.247*	Cd112	n	Cd111m	48.6m	24.1

Table A-3 Contd.

Energy	Target	Reaction	Product	Half-Life	Intensity times Abundance %
0.265	Cd113	2n	Cd111m	48.6m	12.3
	Se76	n_1	Se75	120d	5.4
0.268	Ba135		Ba135m	28.7h	6.7
	Ba136	n	Ba135m	28.7h	7.8
0.276	Ba134	n	Ba135m	38.9h	2.4
0.279	Hg204	n	Hg203	46d	6.7
	Pb204	n	Pb203	52h	1.5
	Se76	n	Se75	120d	2.3
0.284	Cu63	2n	Cu61	3.4h	8.3
0.320*	Cr52	n	C451	27.8d	8.3
0.335*	Cd116	n	Cd115	53.5h	7.2
0.359*	Se74	n	Se73	7.1h	0.9
0.374	Ca44	p	K43	22.4h	1.8
0.375	Hg200	n	Hg199m	43m	23.1
	Hg201	2n	Hg199m	43m	13.2
0.38	Cu63	2n	Cu61	3.4h	1.7
0.388	Sr87	n_1	Sr87m	2.8h	7.0
	Sr88	n	Sr87m	2.8h	81.7
0.400	Se76	n	Se75	120d	1.1
0.406	Ag107	n	Ag106m	8.4d	11.7
0.422*	Pb204	2n	Pb202m	3.6h	1.3
0.439*	Zn70	n	Zn69m	13.8h	0.6
0.511	C12	n	C11	20.5m	annihilation peak
0.511	Ag107	n	Ag106m	8.4d	46.4
0.514	Sr86	n	Sr85	64.5d	9.9
0.53*	Cd116	n	Cd115	53.5h	2.0
0.559	Se77	p	As76	26.3h	3.2
0.564	Sb123	n	Sb122	2.7d	28.3

Table A-3 Contd.

Energy	Target	Reaction	Product	Half-Life	Intensity times Abundance %
0.58*	Cu63	2n	Cu61	3.4h	1.0
0.596*	As75	n	As74	17.7d	61.8
0.616	Ag107	n	Ag106m	8.4d	10.5
0.619	Ca44	p	K43	22.4h	1.7
0.635*	As75	n	As74	17.7d	14.0
0.655	Cu63	2n	Cu61	3.4h	7.6
0.658	Pb204	2n	Pb202m	3.6h	1.2
0.669	Zn64	n	Zn63	38m	3.9
0.674	Cu63	2n	Cu61	3.4h	2.8
0.686*	Sb123	n	Sb122	2.7d	1.4
0.717*	Ag107	n	Ag106m	8.4d	12.1
0.748*	Ag107	n	Ag106m	8.4d	11.5
0.808*	Ag10-7	n	Ag106m	8.4d	13.0
0.834*	Mn55	n	Mn54	312d	100.0
0.847*	Fe57	p	Mn56	2.6h	2.2
0.94*	Cu63	2n	Cu61	3.4h	1.0
0.961	Pb204	2n	Pb202m	3.6h	1.3
0.962	Zn64	n	Zn63	38m	2.9
0.983*	V50	2n	V48	16.1d	0.2
1.046*	Ag107	n	Ag106m	8.4d	16.1
1.115*	Zn66	n	Zn65	243d	14.2
1.170	Sb121	n	Sb120	5.8d	57.3
1.171	Sb121	n	Sb120	15.9m	0.7
1.297*	Ca48	n	Ca47	4.5d	0.1
	B - decay to		Sc47 (.159 Mev)	3.4d	0.1
1.31*	V50	2n	V48	16.1d	0.2

Table A-3 Contd.

Energy	Target	Reaction	Product	Half-Life	Intensity times Abundance %
1.369*	Mg25	p	Na24	15.0h	9.9
1.378*	Ni58	n	Ni57	36h	58.2
1.528*	Ag107	n	Ag106m	8.4d	10.5
1.811*	Fe57	p	Mn56	2.6h	0.6
1.919*	Ni58	n	Ni57	36h	9.5
2.110*	Fe57	p	Mn56	2.6h	0.3
2.754*	Mg25	p	Na24	15.0h	9.9

* Interference free reactions

LIST OF REFERENCES

1. Hislop, J. S., "PAA of Biological and Environmental Samples: A Review", Proceedings of an International Conference, California, V. II, p. 1159-1170, B. L. Berman, Ed., Lawrence Livermore Laboratory, 1973.

2. Andersen, G. H., Graber, F. M., Guinn, V. P., Lukens, H. R. and Settle, D. M., "Nuclear Techniques in the Life Sciences", Proceedings of A symposium, Amsterdam, 1967, IAEA, Vienna, 1967.

3. Azuma, T., Sata, Y., Turugi, R. M. and Kondon, Y., "Anniv. Rep. Radiat. Center", Osaka Prefect, V. 9, No. 26, 1968.

4. General Dynamics Corporation Report CA-7041, No Title, by D. E. Bryan, V. P. Guinn and D. M. Settle, 1966.

5. Modern Trends in Activation Analysis, DeVoe, J. R., Ed., National Bureau of Standards Special Publication 312, Vol. II, 1969.

6. Koch, R. C., Activation Analysis Handbook, Academic Press, 1960.

7. Del Bianco, W., Photonuclear Activation by 20 MeV Gamma Rays, Ph.D. Thesis, University of Pennsylvania, 1961.

8. Lutz, G. J., "Photon Activation Analysis--A Review", Analytical Chemistry, V. 43, No. 1, p. 93-103, January 1971.

9. Naval Research Laboratory Report 7554, Photonuclear Activation Analysis with Ge(Li) Detectors, by M. Elaine Toms, 20 February 1973.

10. Naval Research Laboratory Report 7591, Photonuclear Activation Analysis with Ge(Li) Detectors, Compilation II, by M. Elaine Toms, 9 May 1973.

11. Engelmann, C., "Photon Activation Analysis", Advances in Activation Analysis, p. 1-55, Lenihan, J. M. A., Thomson, S. J. and Guinn, V. P., editors, Academic Press, 1972.

12. Chattopadhyay, A. and Jervis, R. E., "Multielement Determination in Market-Garden Soils by Instrumental Photon Activation Analysis", Analytical Chemistry, V. 46, No. 12, October 1974.

13. Kruger, P., Principles of Activation Analysis, Wiley, 1971.

14. Patterson, H. W. and Thomas, R. H., Accelerator Health Physics, Academic Press, 1973.

15. Aras, N. K., Zoller, W. H., Gordon, G. E. and Lutz, G. J., "Instrumental Photon Activation Analysis of Atmospheric Particulate Material", Analytical Chemistry, V. 45, No. 8, p. 1481-1489, July 1973.

16. Lutz, G. J., "Calculation of Sensitivities in Photon Activation Analysis", Analytical Chemistry, V. 41, No. 3, p. 424-427, March 1969.

17. Gulf Radiation Technology Report Gulf-RT-A-106e4, Development of Nuclear Analytical Techniques for Oil-Slick Identification, Phase IIA, Final Report, 11 June 1971.

18. Schmidt, P. F., Fuel Oil Manual, Industrial Press, Inc., 1969.

19. Von Lehmden, C. J., Jungers, R. H. and Lee, Jr., R. E., "Determination of Trace Elements in Coal, Fly Ash, Fuel Oil, and Gasoline--A Preliminary Comparison of Selected Analytical Techniques", Analytical Chemistry, V. 46, No. 2, p. 239-245, February 1974.

20. Lutz, G. J. and DeSoete, D. A., "Determination of Carbon in Sodium by Photon Activation Analysis", Analytical Chemistry, V. 40, No. 4, p. 820-822, April 1968.

21. Kaminishi, T. and Kojima, C., Japenese Journal of Applied Physics, V. 2, p. 399, 1963.

22. Mulvey, P. F., Jr., Cardarelli, J. A., Zoukis, M., Cooper, R. D. and Burrows, B. A., Article in Journal of Nuclear Medicine, V. 7,. p. 603, 1966.

23. Wilkniss, P. E. and Linnenbom, V. J., Article in Limnol. Oceanog., V. 7, p. 603, 1966.

24. Ricci, E., "Sensitivities for Photon Activation Analysis with Thick Target, 110-MeV Electron Bremsstrahlung", Analytical Chemistry, V. 46, No. 4, p. 615-619, April 1974.

25. Berman, B. L. and Fultz, S. C., "Measurements of the Giant Dipole Resonance with Monoenergetic Photons", Reviews of Modern Physics, V. 47, No. 3, p. 713-761, July 1975.

26. Crouthamel, C. E., Applied Gamma-Ray Spectrometry, Pergamon Press, 1970.

27. ORTEC Inc., Experiments in Nuclear Science, 2d Edition, 1976.

BIBLIOGRAPHY

Bowen, H. J. M.. and Gibbons, D., Radioactivation Analysis, Oxford, 1963.

Instruction Manual for Oil-Slick Identification by Trace Element Patterns Measured with NAA, Gulf Radiation Technology, San Diego, California, 30 May 1972.

MacGregor, M. H., "Linear Accelerators as Radioisotope Producers", Nucleonics, V. 15, No. 11, p. 176-180, November 1957.

Masumoto, K., Kato, T. and Suzuki, N., "Activation Yield Curves of Photonuclear Reactions for Multielement Photon Activation Analysis", Nuclear Instruments and Methods, V. 157, p. 567-577, 1978.

Milner, O. I., Analysis of Petroleum for Trace Elements, MacMillan, 1963.

Naval Research Laboratory Report 7109, Survey on Photon Activation Analysis Using the NRL Linac, by W. L. Bendel and S. K. Numrich, 29 June 1970.

Rakovic, M., Activation Analysis, CRC Press, 1970.

UKAEA Atomic Energy Establishment Report AERE-R-7873, High Resolution Gamma Spectra of 40 to 44 MeV Gamma Photon Activation Products . Part 1 . The Elements Sodium to Molybdenum,. by P. Anderson, J. S. Hislop and D. R. Williams, September 1974.

UKAEA Atomic Energy Establishment Report AERE-R-9022, High Resolution Gamma Spectra of 40-44 MeV Gamma Photoactivation Products: Part 3--A Summary of Gamma Rays, Radionuclides and Nuclear Interferences Observed, by D. R. Williams and J. S. Hislop, September 1980.

INITIAL DISTRIBUTION LIST

		No. Copies
1.	Defense Technical Information Center Cameron Station Alexandria, Virginia 22314	2
2.	Library, Code 0142 Naval Postgraduate School Monterey, California 93940	2
3.	Department Chairman, Code 61DY Department of Physics Naval Postgraduate School Monterey, California 93940	1
4.	Professor F. R. Buskirk, Code 61BS Department of Physics Naval Postgraduate School Monterey, California 93940	3
5.	Lt. Wayne A. Fisher 2722 E. Jefferson St. Baltimore, Maryland 21205	3
6.	Commandant, G-PTE-1/TPU1 U. S. Coast Guard Navy Yard Washington, D. C. 20593	2
7.	Commandant (G-WPE-5) U. S. Coast Guard Bldg. 159-E, Navy Yard Annex Washington, D. C. 20593	1
8.	USCG R & D Center Avery Point Attn: Prof. Bentz Groton, Conn. 06340	1
9.	Major Robert Cooke 1042 Innsbruck St. Livermore, California 94550	1

199592

Thesis
F4675
c.1

Fisher

Instrumental photon activation analysis using the linear accelerator at the Naval Postgraduate